AIMS Mathematics

https://www.aimspress.com/journal/Math

AIMS Mathematics, 10(7): 17248–17273.
DOI: 10.3934/math.2025771
Received: 16 June 2025
Revised: 23 July 2025
Accepted: 28 July 2025
Published: 31 July 2025

Research article

Retrieval of solitons in birefringent optical fibers in communication systems with the effect of conformable fractional derivative using an analytic approach

Altaf Alshuhail[1], Hamdy M. Ahmed[2], Abeer S. Khalifa[3,*], Wael W. Mohammed[1], Mohamed S Algolam[1], Athar I Ahmed[1] and Karim K. Ahmed[4]

[1] Department of Mathematics, College of Science, University of Ha'il, Ha'il 2440, Saudi Arabia

[2] Department of Physics and Engineering Mathematics, Higher Institute of Engineering, El Shorouk Academy, El Shorouk City, Cairo, Egypt

[3] Department of Mathematics, Faculty of Basic Sciences, The German University in Cairo (GUC), Cairo, Egypt

[4] Department of Mathematics, Faculty of Engineering, German International University (GIU), New Administrative Capital, Cairo, Egypt

* **Correspondence:** Email: abeer.kh87@gmail.com.

Abstract: This work is the first to study the concatenation model with conformable fractional derivatives in birefringent fibres, and we give a rich spectrum of optical soliton solutions and many other exact solutions. This concatenation model describes the propagation of solitons in birefringent optical fibres. To achieve this retrieval, the improved modified extended (IME) tanh function technique is utilized, an integration method that generates several soliton solutions and numerous additional solutions. The method captures complicated nonlinear dynamics with greater flexibility than traditional models, providing new insights into pulse propagation characteristics in current optical communication systems. The emergence of soliton solutions automatically determines the respective parameter conditions, which can be easily derived from the types of solution. Outcomes produce a variety of wave forms like bright, dark, and singular solitons, exponential, rational, singular periodic, Jacobi elliptic function solutions, and others. Additionally, the solutions found are utilized to produce a number of interesting 2D and 3D graphs.

Keywords: solitons; NLPDEs; IME tanh function algorithm; concatenation; birefringence; conformable fractional derivatives
Mathematics Subject Classification: 35R11, 35C05, 35C07, 35C08

1. Introduction

Examining traveling wave solutions for nonlinear partial differential equations (NLPDEs) is essential for comprehending the inner workings of complicated processes. Over the past few decades, significant advancements have been made in the fields of electromagnetism, mechanics of liquids, complex physics, atomic materials, electrical engineering, and optical fibers, among others, and numerous effective and proficient techniques for obtaining analytical traveling wave solutions have been discovered in the literature [1–3]. A few recent studies have made substantial contributions towards nonlinear wave dynamics theory employing analytical methods. Ali et al. [4] examined the solitary wave solutions of the reduced modified Camassa–Holm (MCH) and combined KdV–mKdV equations, extending the theory of integrable systems. Ahmed et al. conducted research on a fourth-order (2+1)-dimensional nonlinear Schrödinger equation with a modified extended direct algebraic method that generated a variety of optical soliton solutions [5]. In the meantime, Wang et al. investigated the soliton fission and fusion phenomena in a high-order coupled nonlinear Schrödinger model for the purpose of modeling pulse dynamics in fiber lasers [6]. As a consequence, a number of mathematicians and physicists attempted to devise different techniques to find solutions to these kinds of equations. Soliton theory is important for many nonlinear models when it comes to explaining many intricate events in the field of NLPDEs. Soliton dynamics in various models have been researched by many scientists [7, 8]. Recent investigations have extensively reported the physics of optical solitons in various nonlinear media and fiber geometries. One-soliton solution propagation in multimode optical fibers, taking the impact of higher-order terms to simulate actual transmission conditions, has been investigated by Zhou et al. [9]. Authors in [10] have investigated the dynamics of solitons in magneto-optic waveguides under Kudryashov's law using a modified extended mapping technique to take into account a coupled generalized NLS system. Khalifa et al. [11] studied solitons of twin-core optical couplers under Kerr nonlinearity using the modified extended direct algebraic method to yield a family of exact solutions. In [12], they retrieved soliton solutions of fiber Bragg gratings for arbitrarily high-order coupled systems with arbitrary refractive index profiles, highlighting control of soliton dynamics in complex media. Earlier, Zhou et al. discussed optical solitons in parabolic law nonlinear birefringent fibers and presented observations on the effects of polarization along with non-Kerr-type nonlinearities [13].

Recent research has explored various aspects of nonlinear wave dynamics, focusing particularly on rogue waves and soliton structures in extended (2+1)-dimensional frameworks, including models like the modified Korteweg–de Vries–Calogero–Bogoyavlenskii–Schiff equation [14]. Ahmad et al. [15] explored soliton and lump solutions of the M-truncated stochastic Biswas–Arshed model of interest to optical communications systems, providing insight into the stochastic behavior of nonlinear waves in optical fibers. Shakeel et al. [16] initially employed the modified exp-function method to obtain analytical solutions of the strain wave equation, adding to the study of wave propagation in nonlinear elastic media. Ma and Chen [17] employed a direct search method to obtain accurate analytical solutions of the nonlinear Schrödinger equation and provided new insights into soliton dynamics through the use of symbolic computation techniques. In another paper, Ma and Lee [18] suggested an approach involving a transformed rational function for obtaining exact solutions of the (3+1)-dimensional Jimbo–Miwa equation, which revealed the effectiveness of the method in solving higher-dimensional nonlinear evolution equations.

The concatenation model is an interesting theory that was initially proposed by Ankiewicz et al. in 2014, around ten years ago, even though there are other ideas that explain how solitons move across continents and seas using optical fiber [19, 20]. This model describes the dynamics of soliton transmission at intercontinental distances and combines three well-known equations. These are the Lakshmanan–Porsezian–Daniel (LPD) model, the Sasa–Satsuma equation (SSE), and the nonlinear Schrödinger equation (NLSE). The phrase describes the sequence in which these three models are combined.

The studied concatenation model has recently become even more significant and garnered a lot of interest from a variety of viewpoints. The Laplace–Adomian decomposition approach [21] was also used to numerically address the model. Painleve analysis and the trial equation technique were also used [22–24]. All of these investigations were carried out on the model's scalar form. The last few years have seen major advancements in the research of NLPDEs of water wave models in [25] using the Lie symmetry algorithm. The generalized (3+1) dimensional cubic quasi-linear Schrödinger equation with certain spatial distribution parameters was solved mathematically precisely by Kumar et al. [26] using space-time periodic traveling wave solutions. Bulut et al. [27] used the potent Sine-Gordon expansion approach to look for solutions to several significant nonlinear mathematical models that emerge in nonlinear sciences. The soliton solutions with dual-power law non-linearity and fourth-order dispersion to the nonlinear Schrödinger equation were studied by Zayed et al. [28], and many various investigations were done on different models [29–31].

1.1. Novelty and contribution of the present work

The novelty of this work lies in the application of conformable fractional derivative in birefringent optical fibers so that wave propagation in nonlinear optical media can be modeled more extensively and realistically. In contrast to other classical integer-order approaches, the conformable fractional derivative preserves essential properties like linearity and the chain rule, which are particularly beneficial for analytic solution methods. With the application of the IME tanh function approach to this fractionalized model, we can retrieve a broad class of soliton solutions from bright, dark, and singular waveforms, some of which previously went undocumented in the literature within the case of birefringent fibers. This generalized solution paradigm not only advances the mathematical theory, but also provides new tools for the optimization of signal stability and transmission in future optical communications.

The following is the structure of our article: Section 1 delivers an introduction to the solitons and NLPDEs theory. Section 2 provides an overview of the proposed model along with an explanation of its theoretical background. Given in Section 3, these are the prominent features of the IME tanh function algorithm. In addition, we give the mathematical background of the conformable fractional derivative. To obtain these few classes of exact solutions, a comprehensive symbolic computation is performed using the Wolfram Mathematica program, which summarizes all of the results in Section 4. Section 5 uses both 2D and 3D simulations to graphically depict the dynamic wave patterns of several distinct soliton solutions. Section 6 presents a comparison with some literature. Finally, Section 7 presents the conclusions of the work, and some future perspectives are presented in Section 8.

2. Governing model and theoretical background

For polarization-preserving fibers, the concatenation model may be expressed as follows [32]:

$$\begin{aligned} &i\,\mathcal{U}_t + a\,\mathcal{U}_{xx} + b\,|\mathcal{U}|^2\mathcal{U} + c_1\Big[\sigma_1\,\mathcal{U}_{xxxx} + \sigma_2\,(\mathcal{U}_x)^2\mathcal{U}^* + \sigma_3\,|\mathcal{U}_x|^2\mathcal{U} + \sigma_4\,|\mathcal{U}|^2\mathcal{U}_{xx} + \sigma_5\,\mathcal{U}^2\mathcal{U}^*_{xx} \\ &\quad +\sigma_6|\mathcal{U}|^4\mathcal{U}\Big] + i\,c_2\Big[\sigma_7\,\mathcal{U}_{xxx} + \sigma_8\,|\mathcal{U}|^2\mathcal{U}_x + \sigma_9\,\mathcal{U}^2\mathcal{U}^*_x\Big] = 0. \end{aligned} \tag{2.1}$$

Three well-researched fiber optic models, the NLSE, the LPD equation, and the SSE, are combined to create the concatenation model, or Equation (2.1). It should be mentioned that we have the NLSE when $c_1 = c_2 = 0$, the SSE when $c_1 = 0$, and the LPD model when $c_2 = 0$. Eq (2.1) is the outcome of concatenating the three globally accepted models from nonlinear fiber optics.

In the case of birefringent fibers, Eq (2.1) could be split into the subsequent coupled system of equations [32]:

$$\begin{aligned} &i\frac{\partial^\alpha\Phi}{\partial t^\alpha} + \mathbf{a}_1\Phi_{xx} + \left(\mathbf{b}_1|\Phi|^2 + \mathbf{c}_1|\Psi|^2\right)\Phi + \mathbf{c}_{11}\Big[\sigma_{11}\Phi_{xxxx} + \left(\mathcal{A}_1\Phi_x^2 + \mathcal{B}_1\Psi_x^2\right)\Phi^* + \left(\gamma_1\,|\Phi_x|^2 + \lambda_1\,|\Psi_x|^2\right)\Phi \\ &\quad + \left(\delta_1|\Phi|^2 + \zeta_1|\Psi|^2\right)\Phi_{xx} + \left(\mu_1\Phi^2 + \rho_1\Psi^2\right)\Phi^*_{xx} + \left(\mathbf{f}_1|\Phi|^4 + \mathbf{g}_1|\Phi|^2|\Psi|^2 + \mathbf{h}_1|\Psi|^4\right)\Phi\Big] \\ &\quad +i\,\mathbf{c}_{21}\Big[\sigma_{71}\Phi_{xxx} + \left(\eta_1|\Phi|^2 + \theta_1|\Psi|^2\right)\Phi_x + \left(\varepsilon_1\Phi^2 + \mathcal{T}_1\Psi^2\right)\Phi^*_x\Big] = 0, \end{aligned} \tag{2.2}$$

$$\begin{aligned} &i\frac{\partial^\alpha\Psi}{\partial t^\alpha} + \mathbf{a}_2\Psi_{xx} + \left(\mathbf{b}_2|\Psi|^2 + \mathbf{c}_2|\Phi|^2\right)\Psi + \mathbf{c}_{12}\Big[\sigma_{12}\Psi_{xxxx} + \left(\mathcal{A}_2\Psi_x^2 + \mathcal{B}_2\Phi_x^2\right)\Psi^* + \left(\gamma_2\,|\Psi_x|^2 + \lambda_2\,|\Phi_x|^2\right)\Psi \\ &\quad + \left(\delta_2|\Psi|^2 + \zeta_2|\Phi|^2\right)\Psi_{xx} + \left(\mu_2\Psi^2 + \rho_2\Phi^2\right)\Psi^*_{xx} + \left(\mathbf{f}_2|\Psi|^4 + \mathbf{g}_2|\Psi|^2|\Phi|^2 + \mathbf{h}_2|\Phi|^4\right)\Psi\Big] \\ &\quad +i\,\mathbf{c}_{22}\Big[\sigma_{72}\Psi_{xxx} + \left(\eta_2|\Psi|^2 + \theta_2|\Phi|^2\right)\Psi_x + \left(\varepsilon_2\Psi^2 + \mathcal{T}_2\Phi^2\right)\Psi^*_x\Big] = 0, \end{aligned} \tag{2.3}$$

where $\frac{\partial^\alpha}{\partial t^\alpha}$ is the conformable fractional derivative with order $0 < \alpha \leq 1$, $\Phi(x,t)$ and $\Psi(x,t)$ denote the soliton wave profiles, $\mathbf{a}_j$ $(j = 1,2)$ represent the chromatic dispersion along the two components, $\mathbf{b}_j$ denote self-phase modulation, and $\mathbf{c}_j$ represent the cross-phase modulation. On the other hand, σ_{1j} accounts for the 4th-order dispersions along the two components. Then, $\mathcal{A}_j, \mathcal{B}_j, \gamma_j, \lambda_j, \delta_j, \zeta_j, \mu_j, \rho_j, \mathbf{f}_j, \mathbf{g}_j$, and $\mathbf{h}_j$ are the respective split-ups of the coefficients σ_2 to σ_6 from the LPD model described in Eq (2.1) along the two components for a birefringent fiber. Also, σ_{7j} $(j = 1,2)$ represent the coefficients of the 4th-order dispersion along the components, while in Eq (2.1) this influence is denoted by σ_7. Finally, the components of soliton self-frequency shift along the two components of a birefringent fiber are specified as $\eta_j, \theta_j, \varepsilon_j$, and $\mathcal{T}_j$. These components replaced σ_8 and σ_9 in the SSE part of Eq (2.1).

2.1. Motivations about the suggested model

The aforementioned linked system explains how solitons move through birefringent fibers. The three main equations that comprise it are the NLSE, the LPD model, and the SSE. Concatenating these three models creates a more complete model that can explain how solitons behave in a variety of scenarios. A key formula in nonlinear optics, the NLSE describes how light travels through a material having a nonlinear refractive index. It is employed to simulate how solitons move across fiber optic communication networks. A modified version of the NLSE, the LPD model has extra terms to take into consideration the effects of birefringence, the characteristic of a medium that splits light into two polarized components.

Soliton behavior in birefringent fibers is investigated using this model. Soliton propagation in dispersive media is described by the SSE, another crucial equation in soliton theory. This variant of the NLSE is used to study the behavior of solitons in media with higher-order dispersion. A more comprehensive and accurate description of the behavior of solitons in birefringent optical fibers is provided by the concatenation model, which integrates all three equations into a single model. It has several applications in fiber optic communication systems, which use solitons to transmit data across long distances with little distortion.

This integrated model is designed to phenomenologically explain rich nonlinear dynamics in birefringent fibers, particularly under conditions of ultrashort pulse propagation, high peak powers, and strong birefringence effects. These conditions apply to experimentally applied femtosecond laser systems, polarization-preserving photonic crystal fibers, or dispersion-managed birefringent waveguides where higher-order dispersion, retarded nonlinear response, and birefringence-induced polarization dynamics are involved.

Therefore, this hybrid is an experimentally feasible, physically meaningful model and can explain experimentally observed phenomena such as polarization-dependent pulse splitting, soliton trapping, and birefringent pulse compression or broadening in nonlinear dual-core or highly birefringent fibers.

It should be mentioned that the initial model was presented around ten years ago in [19, 20]. The precise shape of an optical fiber and the applications for which it would be appropriate are still unknown. For the first time, the governing model (2.1) is separated and considered with differential group delay in this study, assuming that it would be logical for erbium-doped fiber. Prior to any laboratory testing, this model is put up as merely analytical. This model was studied before in [32], but in its general form, in this paper, we will study it in its fractional form by applying the conformable fractional derivative.

3. Some mathematical preliminaries

3.1. Mathematical background of the conformable fractional derivatives

Let $v : [0, \infty) \to \mathbb{R}$ exist. Consequently, the conformable fractional derivative for v with order α is as follows [33]:

$$D^{\alpha}v(t) = \lim_{\mathcal{S}\to 0} \frac{v(t + \mathcal{S}^{1-\alpha}) - v(t)}{\mathcal{S}}, \tag{3.1}$$

where $t > 0$, $0 < \alpha \leq 1$.
If v is $\alpha-$differentiable in some interval $(0, \alpha)$, $\alpha > 0$, and

$$\lim_{t\to 0^+} D^{\alpha}v(t)$$

exists, then it could be defined as

$$D^{\alpha}v(0) = \lim_{t\to 0^+} D^{\alpha}v(t). \tag{3.2}$$

The following practical theorem follows from the previous statement [34, 35].

Theorem 1. Assuming $0 < \alpha \leq 1$ and that v and q are $\alpha-$differentiable at $t > 0$, then:

(1) $D^{\alpha}(mv + nq) = m(D^{\alpha}v) + n(D^{\alpha}q), \forall m, n \in \mathbb{R}$.
(2) $D^{\alpha}(t^{g}) = g\, t^{g-\alpha}, \forall g \in \mathbb{R}$.
(3) $D^{\alpha}(\gamma) = 0$ for every constant function, $v(t) = \gamma$.
(4) $D^{\alpha}(vq) = v(D^{\alpha}q) + q(D^{\alpha}v)$.
(5) $D^{\alpha}\left(\dfrac{v}{q}\right) = \dfrac{q(D^{\alpha}v) - v(D^{\alpha}q)}{q^{2}}$.
(6) If v is differentiable, then $(D^{\alpha}v)(t) = t^{1-\alpha}\dfrac{dv}{dt}(t)$.

The conformable fractional derivative is employed due to its tractability, locality, and retention of the conventional calculus rules (product rule, chain rule, and quotient rule), in contrast to Caputo or Riemann–Liouville derivatives, which would complicate analytical solutions. Additionally, it provides a simpler analytical treatment of nonlinear equations whereby the exact closed-form solutions, inclusive of solitons, can be derived. While Caputo and Riemann–Liouville are properly defined, they may be more involved (e.g., requiring initial conditions in integral form or having non-local memory kernels), which could hamper physical interpretation for models of optical fibers. Therefore, in the context of the proposed analytical approach, the conformable derivative is a reasonable compromise between mathematical rigor and physical significance.

3.2. Preliminaries of the IME tanh function algorithm

The application of the IME tanh method to the present nonlinear coupled system is based on a series of assumptions and approximations that make the model amenable analytically. The system is first assumed to have traveling wave solutions, which will enable the use of a wave transformation to reduce the original set of NLPDEs to a single nonlinear ordinary differential equation (NLODE). This form change is based on the assumption that the wave possesses a coherent profile during propagation, which is a typical feature of solitonic propagation in optical fiber. Besides, applying the IME tanh method requires the nonlinear terms to be presentable as polynomial functions of the solution and its derivatives, such that there must be a balance between the highest-order derivative and the nonlinear terms, which is referred to as the homogeneous balance principle. This is an assumption that restricts the admissible forms of nonlinearity to those that are compatible with the ansatz employed by the IME tanh method.

The methodology further stipulates that the system is not chaotic or very disordered in its dynamics in the solution regime, thereby enabling the exclusion of higher-order dispersive and stochastic perturbations unless they are explicitly added (e.g., in conformable or fractional stochastic frameworks). The fractional derivative, which is employed in some of the models, is used because it is easy and chain-rule friendly, which is necessary to preserve analytical tractability when transforming waves. These approximations collectively allow closed-form soliton solutions to be derived while preserving the nonlinear and dispersive leading-order terms of the physical system of interest. For partial differential equations solutions, the IME tanh function algorithm is a helpful tool. It can handle complex boundary conditions, and offers accurate and efficient solutions for both linear and nonlinear equations. It also provides easy-to-understand and easy-to-use solutions. It helps to explain the underlying occurrences by offering a comprehensible physical explanation of the solutions.

This subsection outlines the key elements of the IME tanh function algorithm that will be used in this investigation.

Let us examine the subsequent NLPDE [36]:

$$\mathcal{P}\left(Q, \frac{\partial^\alpha Q}{\partial t^\alpha}, Q_x, Q_{xx}, Q_{tt}, Q_{xt}, \ldots\right) = 0, \tag{3.3}$$

where $\mathcal{P}$ denotes a function in the argument $Q(x,t)$ accompanied by its partial derivatives. The following steps show the detailed algorithm.

I. Here, our goal is to change Eq (3.3), an NLPDE, into an NLODE. To do this, we use the next transformation [17]:

$$Q(x,t) = \mathcal{V}(\xi)e^{i(\kappa x - \ell t)}, \qquad \xi = qx - \omega t. \tag{3.4}$$

The amplitude component of the solution is indicated by $\mathcal{V}(\xi)$ in this case, and the real constants κ, ℓ, q, and ω will be computed as tasks proceed.

We then construct the required NLODE by combining Eq (3.4) in Eq (3.3) as follows:

$$\mathcal{S}(\mathcal{V}, \mathcal{V}', \mathcal{V}'', \mathcal{V}''', \ldots) = 0, \qquad ' = \frac{d}{d\xi}. \tag{3.5}$$

II. Based on the implemented algorithm, the general form of the solution for Eq (3.5) is as follows [18]:

$$\mathcal{V}(\xi) = \sum_{j=0}^{\mathbb{M}} \mathcal{A}_j \mathcal{W}^j(\xi) + \sum_{j=1}^{\mathbb{M}} \mathcal{B}_j \mathcal{W}^{-j}(\xi). \tag{3.6}$$

In this case, the parameters $\mathcal{A}_j$ and $\mathcal{B}_j$ $(j = 1, 2, ..., \mathbb{M})$ represent constants in the resulting solution equation. This gives the necessary condition that $\mathcal{A}_\mathbb{M}$ and $\mathcal{B}_\mathbb{M}$ cannot both be zero simultaneously.

III. To assess the positive integer $\mathbb{M}$, the balancing principle is employed to Eq (3.5). And, the function $\mathcal{W}(\xi)$ also satisfies the following constraint:

$$(\mathcal{W}'(\xi))^2 = \left(\frac{d\mathcal{W}}{d\xi}\right)^2 = \tau_0 + \tau_1\mathcal{W}(\xi) + \tau_2\mathcal{W}^2(\xi) + \tau_3\mathcal{W}^3(\xi) + \tau_4\mathcal{W}^4(\xi), \tag{3.7}$$

while τ_l $(0 \le l \le 4)$ represent constant values that shall assist in identifying potential solution scenarios. From the different possible values of $\tau_0, \tau_1, \tau_2, \tau_3$, and τ_4, we obtain from (3.7) the various kinds of fundamental solutions as follows:

Case 1. $\tau_0 = \tau_1 = \tau_3 = 0$,

$$\mathcal{W}(\xi) = \sqrt{-\frac{\tau_2}{\tau_4}}\,\mathrm{sech}(\sqrt{\tau_2}\,\xi), \qquad \tau_2 > 0, \tau_4 < 0,$$

$$\mathcal{W}(\xi) = \sqrt{-\frac{\tau_2}{\tau_4}}\,\sec(\sqrt{-\tau_2}\,\xi), \qquad \tau_2 < 0, \tau_4 > 0,$$

$$\mathcal{W}(\xi) = \frac{-1}{\sqrt{\tau_4}\,\xi}, \qquad \tau_2 = 0, \tau_4 > 0.$$

Case 2. $\tau_1 = \tau_3 = 0$,

$$\mathcal{W}(\xi) = \varepsilon\sqrt{-\frac{\tau_2}{2\tau_4}}\tanh\left(\sqrt{-\frac{\tau_2}{2}}\,\xi\right), \qquad \tau_2 < 0, \tau_4 > 0, \tau_0 = \frac{\tau_2^2}{4\tau_4},$$

$$\mathcal{W}(\xi) = \varepsilon \sqrt{\frac{\tau_2}{2\tau_4}} \tan\left(\sqrt{\frac{\tau_2}{2}}\, \xi\right), \qquad \tau_2 > 0, \tau_4 > 0, \tau_0 = \frac{\tau_2^2}{4\tau_4},$$

$$\mathcal{W}(\xi) = \sqrt{\frac{-\tau_2 m^2}{\tau_4(2m^2-1)}} \operatorname{cn}\left(\sqrt{\frac{\tau_2}{2m^2-1}}\, \xi\right), \qquad \tau_2 > 0, \tau_4 < 0, \tau_0 = \frac{\tau_2^2 m^2(1-m^2)}{\tau_4(2m^2-1)^2},$$

$$\mathcal{W}(\xi) = \sqrt{\frac{-m^2}{\tau_4(2-m^2)}} \operatorname{dn}\left(\sqrt{\frac{\tau_2}{2-m^2}}\, \xi\right), \qquad \tau_2 > 0, \tau_4 < 0, \tau_0 = \frac{\tau_2^2(1-m^2)}{\tau_4(2-m^2)^2},$$

$$\mathcal{W}(\xi) = \varepsilon \sqrt{-\frac{\tau_2 m^2}{\tau_4(1+m^2)}} \operatorname{sn}\left(\sqrt{-\frac{\tau_2}{1+m^2}}\, \xi\right), \qquad \tau_2 < 0, \tau_4 > 0, \tau_0 = \frac{\tau_2^2 m^2}{\tau_4(m^2+1)^2},$$

where m is the modulus of the Jacobi elliptic functions.
Case 3. $\tau_3 = \tau_4 = 0$,

$$\mathcal{W}(\xi) = -\frac{\tau_1}{2\tau_2} + \exp(\varepsilon \sqrt{\tau_2}\, \xi), \qquad \tau_2 > 0, \tau_0 = \frac{\tau_1^2}{4\tau_2},$$

$$\mathcal{W}(\xi) = -\frac{\tau_1}{2\tau_2} + \frac{\varepsilon \tau_1}{2\tau_2} \sin(\sqrt{-\tau_2}\, \xi), \qquad \tau_0 = 0, \tau_2 < 0,$$

$$\mathcal{W}(\xi) = -\frac{\tau_1}{2\tau_2} + \frac{\varepsilon \tau_1}{2\tau_2} \sinh(2\sqrt{\tau_2}\, \xi), \qquad \tau_0 = 0, \tau_2 > 0,$$

$$\mathcal{W}(\xi) = \varepsilon \sqrt{-\frac{\tau_0}{\tau_2}} \sin(\sqrt{-\tau_2}\, \xi), \qquad \tau_1 = 0, \tau_0 > 0, \tau_2 < 0,$$

$$\mathcal{W}(\xi) = \varepsilon \sqrt{\frac{\tau_0}{\tau_2}} \sinh(\sqrt{\tau_2}\, \xi), \qquad \tau_1 = 0, \tau_0 > 0, \tau_2 > 0.$$

IV. Rendering Eq (3.5) with the solution that seems to be provided in Eqs (3.6) and (3.7) will generate a polynomial in $\mathcal{W}(\xi)$. Mathematical software like Wolfram Mathematica or Maple programs may be utilized to solve an algebraic system of nonlinear equations that arises when the coefficients of $\mathcal{W}^k(\xi)$, $(k = 0, \pm 1, \pm 2, ...)$, are set equal to zero. For Eq (3.3), there are thus several exact solutions that we can obtain.

4. Structuring of optical solitons and various exact solutions

In this part, the IME tanh function algorithm is utilized to create some possible solutions for Eqs (2.2) and (2.3). To achieve this, we assume that

$$\Phi(x,t) = \mathbb{P}_1(\xi)\, e^{i\left(-\mathcal{K}x + \omega \frac{t^\alpha}{\alpha} + \theta_0\right)}, \tag{4.1}$$

$$\Psi(x,t) = \mathbb{P}_2(\xi)\, e^{i\left(-\mathcal{K}x + \omega \frac{t^\alpha}{\alpha} + \theta_0\right)}, \tag{4.2}$$

and

$$\xi = \Bbbk\left(x - \frac{t^\alpha}{\alpha}\nu\right), \qquad \nu \neq 0. \tag{4.3}$$

where $\mathbb{P}_1(\xi)$ and $\mathbb{P}_2(\xi)$ denote the amplitude of the solution which are unique for each type of solution, and $\mathcal{K}$, ω, θ_0, $\Bbbk$, and ν represent some constants to be evaluated within the paper. Observe that the use of the wave variable (ξ) here serves to highlight the impact of the fractional derivative on wave propagation. Specifically, the occurrence of the t^α term reflects the impact of a fractional time derivative with $0 < \alpha \leq 1$ modeling sub-diffusive behavior. This fractional exponent reduces the rate of temporal evolution of the wave compared to the classical case ($\alpha = 1$), which shows that the wave speed properly reduces in fractional-order media. This has a physical implication that propagation is a memory process where the response of the medium lags owing to the intrinsic non-locality introduced by the fractional derivative. Thus, for $\alpha < 1$, the wave experiences retardation in transmission behavior, which conforms to anomalous diffusion phenomena often encountered in complex physical systems. It is also known that the velocity is not constant for $\alpha < 0$.

When Eqs (4.1)–(4.3) are substituted into Eqs (2.2) and (2.3), the real and imaginary components are separated to produce the following:

Real parts

$$\begin{aligned}
&-\left[\mathcal{K}^3(\mathbf{c}_{21}\sigma_{71}-\mathbf{c}_{11}\mathcal{K}\sigma_{11})+\mathbf{a}_1\mathcal{K}^2+\omega\right]\mathbb{P}_1+\left[\mathbf{b}_1-\mathbf{c}_{11}\mathcal{K}^2(\mathcal{A}_1-\gamma_1+\delta_1+\mu_1)+\mathbf{c}_{21}\mathcal{K}(\eta_1-\varepsilon_1)\right]\mathbb{P}_1^3\\
&+\mathbf{c}_{11}\mathbf{f}_1\mathbb{P}_1^5+\mathbf{c}_{11}\mathbf{g}_1\mathbb{P}_2^2\,\mathbb{P}_1^3+\mathbf{c}_{11}\mathbf{h}_1\mathbb{P}_2^4\,\mathbb{P}_1+\left[\mathbf{c}_1-\mathcal{K}\left(\mathbf{c}_{11}\mathcal{K}(\mathcal{B}_1+\zeta_1-\lambda_1+\rho_1)+\mathbf{c}_{21}(\mathcal{T}_1-\theta_1)\right)\right]\mathbb{P}_1\mathbb{P}_2^2\\
&+\mathbf{c}_{11}\Bbbk^2(\mathcal{A}_1+\gamma_1)\mathbb{P}_1(\mathbb{P}_1')^2+\mathbf{c}_{11}\Bbbk^2(\mathcal{B}_1+\lambda_1)\mathbb{P}_1(\mathbb{P}_2')^2+\mathbf{c}_{11}\Bbbk^2\left(\mathbb{P}_1^2(\delta_1+\mu_1)+\mathbb{P}_2^2(\zeta_1+\rho_1)\right)\mathbb{P}_1''\\
&+\Bbbk^2\left[\mathbf{a}_1+3\mathcal{K}(\mathbf{c}_{21}\sigma_{71}-2\mathbf{c}_{11}\mathcal{K}\sigma_{11})\right]\mathbb{P}_1''+\mathbf{c}_{11}\sigma_{11}\Bbbk^4\,\mathbb{P}_1^{(4)}=0,
\end{aligned}\tag{4.4}$$

$$\begin{aligned}
&-\left[\mathcal{K}^3(\mathbf{c}_{22}\sigma_{72}-\mathbf{c}_{12}\mathcal{K}\sigma_{12})+\mathbf{a}_2\mathcal{K}^2+\omega\right]\mathbb{P}_2+\left[\mathbf{b}_2-\mathbf{c}_{12}\mathcal{K}^2(\mathcal{A}_2-\gamma_2+\delta_2+\mu_2)+\mathbf{c}_{22}\mathcal{K}(\eta_2-\varepsilon_2)\right]\mathbb{P}_2^3\\
&+\mathbf{c}_{12}\mathbf{f}_2\mathbb{P}_2^5+\mathbf{c}_{12}\mathbf{g}_2\mathbb{P}_1^2\,\mathbb{P}_2^3+\mathbf{c}_{12}\mathbf{h}_2\mathbb{P}_1^4\,\mathbb{P}_2+\left[\mathbf{c}_2-\mathcal{K}\left(\mathbf{c}_{12}\mathcal{K}(\mathcal{B}_2+\zeta_2-\lambda_2+\rho_2)+\mathbf{c}_{22}(\mathcal{T}_2-\theta_2)\right)\right]\mathbb{P}_2\mathbb{P}_1^2\\
&+\mathbf{c}_{12}\Bbbk^2(\mathcal{A}_2+\gamma_2)\mathbb{P}_2(\mathbb{P}_2')^2+\mathbf{c}_{12}\Bbbk^2(\mathcal{B}_2+\lambda_2)\mathbb{P}_2(\mathbb{P}_1')^2+\mathbf{c}_{12}\Bbbk^2\left(\mathbb{P}_2^2(\delta_2+\mu_2)+\mathbb{P}_1^2(\zeta_2+\rho_2)\right)\mathbb{P}_2''\\
&+\Bbbk^2\left[\mathbf{a}_2+3\mathcal{K}(\mathbf{c}_{22}\sigma_{72}-2\mathbf{c}_{12}\mathcal{K}\sigma_{12})\right]\mathbb{P}_2''+\mathbf{c}_{12}\sigma_{12}\Bbbk^4\,\mathbb{P}_2^{(4)}=0,
\end{aligned}\tag{4.5}$$

while the imaginary parts reduce to

$$\begin{aligned}
&-\left[\nu-\left(\mathcal{K}^2(4\mathbf{c}_{11}\mathcal{K}\sigma_{11}-3\mathbf{c}_{21}\sigma_{71})\right)+2\mathbf{a}_1\mathcal{K}\right]\mathbb{P}_1'+\left[\mathbf{c}_{21}(\varepsilon_1+\eta_1)-2\mathbf{c}_{11}\mathcal{K}(\mathcal{A}_1+\delta_1-\mu_1)\right]\mathbb{P}_1^2\,\mathbb{P}_1'\\
&+\left[\mathbf{c}_{21}(\theta_1+\mathcal{T}_1)-2\mathbf{c}_{11}\mathcal{K}(\zeta_1-\rho_1)\right]\mathbb{P}_2^2\,\mathbb{P}_1'-2\mathcal{B}_1\mathbf{c}_{11}\mathcal{K}\,\mathbb{P}_1\mathbb{P}_2\,\mathbb{P}_2'+\Bbbk^2(\mathbf{c}_{21}\sigma_{71}-4\mathbf{c}_{11}\mathcal{K}\sigma_{11})\mathbb{P}_1^{(3)}=0,
\end{aligned}\tag{4.6}$$

$$\begin{aligned}
&-\left[\nu-\left(\mathcal{K}^2(4\mathbf{c}_{12}\mathcal{K}\sigma_{12}-3\mathbf{c}_{22}\sigma_{72})\right)+2\mathbf{a}_2\mathcal{K}\right]\mathbb{P}_2'+\left[\mathbf{c}_{22}(\varepsilon_2+\eta_2)-2\mathbf{c}_{12}\mathcal{K}(\mathcal{A}_2+\delta_2-\mu_2)\right]\mathbb{P}_2^2\,\mathbb{P}_2'\\
&+\left[\mathbf{c}_{22}(\theta_2+\mathcal{T}_2)-2\mathbf{c}_{12}\mathcal{K}(\zeta_2-\rho_2)\right]\mathbb{P}_1^2\,\mathbb{P}_2'-2\mathcal{B}_2\mathbf{c}_{12}\mathcal{K}\,\mathbb{P}_2\mathbb{P}_1\,\mathbb{P}_1'+\Bbbk^2(\mathbf{c}_{22}\sigma_{72}-4\mathbf{c}_{12}\mathcal{K}\sigma_{12})\mathbb{P}_2^{(3)}=0.
\end{aligned}\tag{4.7}$$

With the following limitations, we can get the exact solution for $j = 1, 2$:

$$\mathbf{c}_{2j}\left(\varepsilon_j+\eta_j\right)=2\mathcal{K}\mathbf{c}_{1j}\left(\mathcal{A}_j+\delta_j-\mu_j\right),\tag{4.8}$$

$$\mathbf{c}_{2j}\left(\theta_j+\mathcal{T}_j\right)=2\mathcal{K}\mathbf{c}_{1j}\left(\zeta_j-\rho_j\right),\tag{4.9}$$

$$\mathcal{B}_j=0,\tag{4.10}$$

$$\mathbf{c}_{2j}\sigma_{7j}=4\mathcal{K}\mathbf{c}_{1j}\sigma_{1j},\tag{4.11}$$

from which one can retrieve the speed as

$$\nu = -2\mathcal{K}\left(\mathbf{a}_j + \mathcal{K}\mathbf{c}_{2j}\sigma_{7j}\right). \tag{4.12}$$

Set

$$\mathbb{P}_2 = \varsigma\,\mathbb{P}_1, \quad \varsigma \neq 0, 1. \tag{4.13}$$

Thus, Eqs (4.4) and (4.5) will be as follows:

$$\begin{aligned}&\left[\mathbf{c}_{11}\mathcal{K}^4\sigma_{11} - \mathbf{c}_{21}\mathcal{K}^3\sigma_{71} - \mathbf{a}_1\mathcal{K}^2 - \omega\right]\mathbb{P}_1 + \Big[\mathbf{b}_1 + \mathbf{c}_1\varsigma^2 - \mathcal{K}\Big(- \mathbf{c}_{21}\theta_1\varsigma^2 + \mathcal{A}_1\mathbf{c}_{11}\mathcal{K} + \mathbf{c}_{11}\mathcal{K}(- \gamma_1 + \delta_1\\&+\varsigma^2(\zeta_1 - \lambda_1 + \rho_1) + \mu_1) + \mathbf{c}_{21}\left(\varepsilon_1 - \eta_1 + \mathcal{T}_1\varsigma^2\right)\Big)\Big]\mathbb{P}_1^3 + \mathbf{c}_{11}\left(\mathbf{f}_1 + \mathbf{g}_1\varsigma^2 + \mathbf{h}_1\varsigma^4\right)\mathbb{P}_1^5 + \mathbf{c}_{11}\mathbb{k}^2\Big(\mathcal{A}_1 + \gamma_1\\&+\lambda_1\varsigma^2\Big)\mathbb{P}_1\left(\mathbb{P}_1'\right)^2 + \mathbf{c}_{11}\mathbb{k}^2\left(\delta_1 + \varsigma^2\left(\zeta_1 + \rho_1\right) + \mu_1\right)\mathbb{P}_1^2\,\mathbb{P}_1'' + \mathbb{k}^2\left[\mathbf{a}_1 + 3\mathcal{K}\left(\mathbf{c}_{21}\sigma_{71} - 2\mathbf{c}_{11}\mathcal{K}\sigma_{11}\right)\right]\mathbb{P}_1''\\&+\mathbf{c}_{11}\mathbb{k}^4\sigma_{11}\mathbb{P}_1^{(4)} = 0,\end{aligned} \tag{4.14}$$

$$\begin{aligned}&\varsigma\left(\mathbf{c}_{12}\mathcal{K}^4\sigma_{12} - \mathbf{c}_{22}\mathcal{K}^3\sigma_{72} - \mathbf{a}_2\mathcal{K}^2 - \omega\right)\mathbb{P}_1 + \varsigma\Big[\mathbf{b}_2\varsigma^2 + \mathbf{c}_2 - \mathcal{K}\Big[\mathbf{c}_{22}\Big(\varsigma^2\left(\varepsilon_2 - \eta_2\right) - \theta_2\Big) + \mathcal{A}_2\mathbf{c}_{12}\mathcal{K}\varsigma^2\\&+\mathbf{c}_{12}\mathcal{K}\left[\varsigma^2\left(-\gamma_2 + \delta_2 + \mu_2\right) + \zeta_2 - \lambda_2 + \rho_2\right] + \mathbf{c}_{22}\mathcal{T}_2\Big]\Big]\mathbb{P}_1^3 + \mathbf{c}_{12}\varsigma\left(\mathbf{f}_2\varsigma^4 + \mathbf{g}_2\varsigma^2 + \mathbf{h}_2\right)\mathbb{P}_1^5\\&+\mathbf{c}_{12}\mathbb{k}^2\varsigma\left(\varsigma^2\left(\mathcal{A}_2 + \gamma_2\right) + \lambda_2\right)\mathbb{P}_1\left(\mathbb{P}_1'\right)^2 + \mathbf{c}_{12}\mathbb{k}^2\varsigma\left(\varsigma^2\left(\delta_2 + \mu_2\right) + \zeta_2 + \rho_2\right)\mathbb{P}_1^2\,\mathbb{P}_1'' + \mathbb{k}^2\varsigma\Big(\mathbf{a}_2\\&+3\mathcal{K}\Big(\mathbf{c}_{22}\sigma_{72} - 2\mathbf{c}_{12}\mathcal{K}\sigma_{12}\Big)\Big)\mathbb{P}_1'' + \mathbf{c}_{12}\mathbb{k}^4\sigma_{12}\varsigma\mathbb{P}_1^{(4)} = 0.\end{aligned} \tag{4.15}$$

Following that, the coefficients of Eqs (4.14) and (4.15) may be found to be comparable using the following constraints:

$$\mathbf{c}_{11}\sigma_{11} = \varsigma\,\mathbf{c}_{12}\sigma_{12}, \tag{4.16}$$

$$\mathbf{a}_1 + 3\mathcal{K}\left(\mathbf{c}_{21}\sigma_{71} - 2\mathbf{c}_{11}\mathcal{K}\sigma_{11}\right) = \varsigma\left(\mathbf{a}_2 + 3\mathcal{K}\left(\mathbf{c}_{22}\sigma_{72} - 2\mathbf{c}_{12}\mathcal{K}\sigma_{12}\right)\right), \tag{4.17}$$

$$\mathbf{c}_{11}\left(\delta_1 + \varsigma^2\left(\zeta_1 + \rho_1\right) + \mu_1\right) = \mathbf{c}_{12}\varsigma\left(\varsigma^2\left(\delta_2 + \mu_2\right) + \zeta_2 + \rho_2\right), \tag{4.18}$$

$$\mathbf{c}_{11}\left(\mathcal{A}_1 + \gamma_1\right) + \mathbf{c}_{11}\lambda_1\varsigma^2 = \varsigma\left(\mathbf{c}_{12}\varsigma^2\left(\mathcal{A}_2 + \gamma_2\right) + \mathbf{c}_{12}\lambda_2\right), \tag{4.19}$$

$$-\left(\mathcal{K}^2\left(\mathbf{a}_1 + \mathcal{K}\left(\mathbf{c}_{21}\sigma_{71} - \mathbf{c}_{11}\mathcal{K}\sigma_{11}\right)\right)\right) - \omega = \varsigma\left(-\left(\mathcal{K}^2\left(\mathbf{a}_2 + \mathcal{K}\left(\mathbf{c}_{22}\sigma_{72} - \mathbf{c}_{12}\mathcal{K}\sigma_{12}\right)\right)\right) - \omega\right), \tag{4.20}$$

$$\begin{aligned}&\mathbf{b}_1 - \mathcal{K}\left(\mathbf{c}_{21}\left(\varepsilon_1 - \eta_1\right) + \mathbf{c}_{11}\mathcal{K}\left(\mathcal{A}_1 - \gamma_1 + \delta_1 + \mu_1\right)\right) + \varsigma^2\left(\mathbf{c}_1 - \mathcal{K}\left(\mathbf{c}_{11}\mathcal{K}\left(\zeta_1 - \lambda_1 + \rho_1\right) + \mathbf{c}_{21}\left(\mathcal{T}_1 - \theta_1\right)\right)\right)\\&= \varsigma\Big(\mathbf{c}_2 + \varsigma^2\left(\mathbf{b}_2 - \mathcal{K}\left(\mathbf{c}_{22}\left(\varepsilon_2 - \eta_2\right) + \mathbf{c}_{12}\mathcal{K}\left(\mathcal{A}_2 - \gamma_2 + \delta_2 + \mu_2\right)\right)\right) - \mathcal{K}\left(\mathbf{c}_{12}\mathcal{K}\left(\zeta_2 - \lambda_2 + \rho_2\right) + \mathbf{c}_{22}\left(\mathcal{T}_2 - \theta_2\right)\right)\Big),\end{aligned} \tag{4.21}$$

and

$$\mathbf{c}_{11}\mathbf{f}_1 + \mathbf{c}_{11}\mathbf{g}_1\varsigma^2 + \mathbf{c}_{11}\mathbf{h}_1\varsigma^4 = \varsigma\left(\mathbf{c}_{12}\mathbf{f}_2\varsigma^4 + \mathbf{c}_{12}\mathbf{g}_2\varsigma^2 + \mathbf{c}_{12}\mathbf{h}_2\right). \tag{4.22}$$

Therefore, we will deal only with Eq (4.14), which will take the following form:

$$\mathbf{c}_{11}\mathbb{k}^4\sigma_{11}\mathbb{P}_1^{(4)} + \mathcal{L}_0\mathbb{P}_1'' + \mathcal{L}_1\mathbb{P}_1^2\,\mathbb{P}_1'' + \mathcal{L}_2\mathbb{P}_1\left(\mathbb{P}_1'\right)^2 + \mathcal{L}_3\mathbb{P}_1 + \mathcal{L}_4\mathbb{P}_1^3 + \mathcal{L}_5\mathbb{P}_1^5 = 0. \tag{4.23}$$

The symbols $\mathcal{L}_i$ and $(i = 0, 1, 2, 3, 4, 5)$ are some constants that are included for notational ease of use:

$$\begin{aligned}\mathcal{L}_0 &= \mathbb{k}^2\left(\mathbf{a}_1 + 3\mathcal{K}\left(\mathbf{c}_{21}\sigma_{71} - 2\mathbf{c}_{11}\mathcal{K}\sigma_{11}\right)\right),\\ \mathcal{L}_1 &= \mathbf{c}_{11}\mathbb{k}^2\left(\delta_1 + \varsigma^2\left(\zeta_1 + \rho_1\right) + \mu_1\right),\\ \mathcal{L}_2 &= \mathbf{c}_{11}\mathbb{k}^2\left(\mathcal{A}_1 + \gamma_1\right) + \mathbf{c}_{11}\lambda_1\mathbb{k}^2\varsigma^2,\\ \mathcal{L}_3 &= -\left(\mathcal{K}^2\left(\mathbf{a}_1 + \mathcal{K}\left(\mathbf{c}_{21}\sigma_{71} - \mathbf{c}_{11}\mathcal{K}\sigma_{11}\right)\right)\right) - \omega,\\ \mathcal{L}_4 &= \mathbf{b}_1 - \mathcal{K}\left(\mathbf{c}_{21}\left(\varepsilon_1 - \eta_1\right) + \mathbf{c}_{11}\mathcal{K}\left(\mathcal{A}_1 - \gamma_1 + \delta_1 + \mu_1\right)\right)\\ &\quad + \varsigma^2\left(\mathbf{c}_1 - \mathcal{K}\left(\mathbf{c}_{11}\mathcal{K}\left(\zeta_1 - \lambda_1 + \rho_1\right) + \mathbf{c}_{21}\left(\mathcal{T}_1 - \theta_1\right)\right)\right),\\ \mathcal{L}_5 &= \mathbf{c}_{11}\mathbf{f}_1 + \mathbf{c}_{11}\mathbf{g}_1\varsigma^2 + \mathbf{c}_{11}\mathbf{h}_1\varsigma^4.\end{aligned} \tag{4.24}$$

Therefore, using the balance principle described in subsection 3.2 between $\mathbb{P}_1^{(4)}$ and $\mathbb{P}_1^5$, one can construct the exact solution of Eq (4.23) as

$$\mathbb{P}_1(\xi) = \mathcal{A}_0 + \mathcal{A}_1\mathcal{W}(\xi) + \frac{\mathcal{B}_1}{\mathcal{W}(\xi)}, \tag{4.25}$$

where $\mathcal{A}_i$ $(i = 0, 1)$ and $\mathcal{B}_1$ are constants, which can be calculated under the restrictions $\mathcal{A}_1 \neq 0$ or $\mathcal{B}_1 \neq 0$.
If the solution form in Eq (4.25) is substituted with the limitation in Eq (3.7) in Eq (4.23), then there exists a polynomial in $\mathcal{W}(\xi)$. Upon adding all terms with identical powers until they reach zero, an algebraic system of nonlinear equations is created:

$$\begin{aligned}
0 &= 2\tau_0\mathcal{L}_1\mathcal{B}_1^3 + \tau_0\mathcal{L}_2\mathcal{B}_1^3 + \mathcal{L}_5\mathcal{B}_1^5 + 24\mathbf{c}_{11}\mathbb{k}^4\sigma_{11}\tau_0^2\mathcal{B}_1,\\
0 &= 4\tau_0\mathcal{L}_1\mathcal{A}_0\mathcal{B}_1^2 + \tau_0\mathcal{L}_2\mathcal{A}_0\mathcal{B}_1^2 + 5\mathcal{L}_5\mathcal{A}_0\mathcal{B}_1^4 + \frac{3}{2}\tau_1\mathcal{L}_1\mathcal{B}_1^3 + \tau_1\mathcal{L}_2\mathcal{B}_1^3 + 30\mathbf{c}_{11}\mathbb{k}^4\sigma_{11}\tau_0\tau_1\mathcal{B}_1,\\
0 &= 4\tau_0\mathcal{L}_1\mathcal{A}_1\mathcal{B}_1^2 - \tau_0\mathcal{L}_2\mathcal{A}_1\mathcal{B}_1^2 + 2\tau_0\mathcal{L}_1\mathcal{A}_0^2\mathcal{B}_1 + 3\tau_1\mathcal{L}_1\mathcal{A}_0\mathcal{B}_1^2 + \tau_1\mathcal{L}_2\mathcal{A}_0\mathcal{B}_1^2 + 5\mathcal{L}_5\mathcal{A}_1\mathcal{B}_1^4 + 10\mathcal{L}_5\mathcal{A}_0^2\mathcal{B}_1^3 + 2\tau_0\mathcal{L}_0\mathcal{B}_1\\
&\quad + \tau_2\mathcal{L}_1\mathcal{B}_1^3 + \tau_2\mathcal{L}_2\mathcal{B}_1^3 + \mathcal{L}_4\mathcal{B}_1^3 + \frac{15}{2}\mathbf{c}_{11}\mathbb{k}^4\sigma_{11}\tau_1^2\mathcal{B}_1 + 20\mathbf{c}_{11}\mathbb{k}^4\sigma_{11}\tau_0\tau_2\mathcal{B}_1,\\
0 &= 4\tau_0\mathcal{L}_1\mathcal{A}_0\mathcal{A}_1\mathcal{B}_1 - 2\tau_0\mathcal{L}_2\mathcal{A}_0\mathcal{A}_1\mathcal{B}_1 + \frac{7}{2}\tau_1\mathcal{L}_1\mathcal{A}_1\mathcal{B}_1^2 - \tau_1\mathcal{L}_2\mathcal{A}_1\mathcal{B}_1^2 + \frac{3}{2}\tau_1\mathcal{L}_1\mathcal{A}_0^2\mathcal{B}_1 + 2\tau_2\mathcal{L}_1\mathcal{A}_0\mathcal{B}_1^2 + \tau_2\mathcal{L}_2\mathcal{A}_0\mathcal{B}_1^2\\
&\quad + 20\mathcal{L}_5\mathcal{A}_0\mathcal{A}_1\mathcal{B}_1^3 + 10\mathcal{L}_5\mathcal{A}_0^3\mathcal{B}_1^2 + 3\mathcal{L}_4\mathcal{A}_0\mathcal{B}_1^2 + \frac{3}{2}\tau_1\mathcal{L}_0\mathcal{B}_1 + \frac{1}{2}\tau_3\mathcal{L}_1\mathcal{B}_1^3 + \tau_3\mathcal{L}_2\mathcal{B}_1^3 + \frac{15}{2}\mathbf{c}_{11}\mathbb{k}^4\sigma_{11}\tau_1\tau_2\mathcal{B}_1\\
&\quad + 15\mathbf{c}_{11}\mathbb{k}^4\sigma_{11}\tau_0\tau_3\mathcal{B}_1,\\
0 &= 2\tau_0\mathcal{L}_1\mathcal{A}_1^2\mathcal{B}_1 - \tau_0\mathcal{L}_2\mathcal{A}_1^2\mathcal{B}_1 + 4\tau_1\mathcal{L}_1\mathcal{A}_0\mathcal{A}_1\mathcal{B}_1 - 2\tau_1\mathcal{L}_2\mathcal{A}_0\mathcal{A}_1\mathcal{B}_1 + 3\tau_2\mathcal{L}_1\mathcal{A}_1\mathcal{B}_1^2 - \tau_2\mathcal{L}_2\mathcal{A}_1\mathcal{B}_1^2 + \tau_2\mathcal{L}_1\mathcal{A}_0^2\mathcal{B}_1\\
&\quad + \tau_3\mathcal{L}_1\mathcal{A}_0\mathcal{B}_1^2 + \tau_3\mathcal{L}_2\mathcal{A}_0\mathcal{B}_1^2 + 10\mathcal{L}_5\mathcal{A}_1^2\mathcal{B}_1^3 + 30\mathcal{L}_5\mathcal{A}_0^2\mathcal{A}_1\mathcal{B}_1^2 + 3\mathcal{L}_4\mathcal{A}_1\mathcal{B}_1^2 + 5\mathcal{L}_5\mathcal{A}_0^4\mathcal{B}_1 + 3\mathcal{L}_4\mathcal{A}_0^2\mathcal{B}_1 + \tau_2\mathcal{L}_0\mathcal{B}_1\\
&\quad + \tau_4\mathcal{L}_2\mathcal{B}_1^3 + \mathcal{L}_3\mathcal{B}_1 + \mathbf{c}_{11}\mathbb{k}^4\sigma_{11}\tau_2^2\mathcal{B}_1 + \frac{9}{2}\mathbf{c}_{11}\mathbb{k}^4\sigma_{11}\tau_1\tau_3\mathcal{B}_1 + 12\mathbf{c}_{11}\mathbb{k}^4\sigma_{11}\tau_0\tau_4\mathcal{B}_1,\\
0 &= \frac{1}{2}\tau_1\mathcal{L}_1\mathcal{A}_1\mathcal{A}_0^2 + \tau_0\mathcal{L}_2\mathcal{A}_1^2\mathcal{A}_0 + \frac{1}{2}\tau_1\mathcal{L}_0\mathcal{A}_1 + \frac{1}{2}\tau_3\mathcal{L}_1\mathcal{A}_0^2\mathcal{B}_1 + 4\tau_2\mathcal{L}_1\mathcal{A}_1\mathcal{A}_0\mathcal{B}_1 - 2\tau_2\mathcal{L}_2\mathcal{A}_1\mathcal{A}_0\mathcal{B}_1 + \tau_4\mathcal{L}_2\mathcal{A}_0\mathcal{B}_1^2\\
&\quad + \frac{5}{2}\tau_1\mathcal{L}_1\mathcal{A}_1^2\mathcal{B}_1 - \tau_1\mathcal{L}_2\mathcal{A}_1^2\mathcal{B}_1 + \frac{5}{2}\tau_3\mathcal{L}_1\mathcal{A}_1\mathcal{B}_1^2 - \tau_3\mathcal{L}_2\mathcal{A}_1\mathcal{B}_1^2 + 20\mathcal{L}_5\mathcal{A}_1\mathcal{A}_0^3\mathcal{B}_1 + 30\mathcal{L}_5\mathcal{A}_1^2\mathcal{A}_0\mathcal{B}_1^2 + 6\mathcal{L}_4\mathcal{A}_1\mathcal{A}_0\mathcal{B}_1\\
&\quad + \mathcal{L}_5\mathcal{A}_0^5 + \mathcal{L}_4\mathcal{A}_0^3 + \mathcal{L}_3\mathcal{A}_0 + \frac{1}{2}\tau_3\mathcal{L}_0\mathcal{B}_1 + \frac{1}{2}\mathbf{c}_{11}\mathbb{k}^4\sigma_{11}\tau_1\tau_2\mathcal{A}_1 + 3\mathbf{c}_{11}\mathbb{k}^4\sigma_{11}\tau_0\tau_3\mathcal{A}_1 + \frac{1}{2}\mathbf{c}_{11}\mathbb{k}^4\sigma_{11}\tau_2\tau_3\mathcal{B}_1\\
&\quad + 3\mathbf{c}_{11}\mathbb{k}^4\sigma_{11}\tau_1\tau_4\mathcal{B}_1,\\
0 &= \tau_0\mathcal{L}_2\mathcal{A}_1^3 + \tau_1\mathcal{L}_1\mathcal{A}_0\mathcal{A}_1^2 + \tau_1\mathcal{L}_2\mathcal{A}_0\mathcal{A}_1^2 + \tau_2\mathcal{L}_1\mathcal{A}_0^2\mathcal{A}_1 + \tau_2\mathcal{L}_0\mathcal{A}_1 + 3\tau_2\mathcal{L}_1\mathcal{A}_1^2\mathcal{B}_1 - \tau_2\mathcal{L}_2\mathcal{A}_1^2\mathcal{B}_1 + 4\tau_3\mathcal{L}_1\mathcal{A}_0\mathcal{A}_1\mathcal{B}_1\\
&\quad - 2\tau_3\mathcal{L}_2\mathcal{A}_0\mathcal{A}_1\mathcal{B}_1 + 2\tau_4\mathcal{L}_1\mathcal{A}_1\mathcal{B}_1^2 - \tau_4\mathcal{L}_2\mathcal{A}_1\mathcal{B}_1^2 + 10\mathcal{L}_5\mathcal{A}_1^3\mathcal{B}_1^2 + 30\mathcal{L}_5\mathcal{A}_0^2\mathcal{A}_1^2\mathcal{B}_1 + 3\mathcal{L}_4\mathcal{A}_1^2\mathcal{B}_1 + 5\mathcal{L}_5\mathcal{A}_0^4\mathcal{A}_1\\
&\quad + 3\mathcal{L}_4\mathcal{A}_0^2\mathcal{A}_1 + \mathcal{L}_3\mathcal{A}_1 + \mathbf{c}_{11}\mathbb{k}^4\sigma_{11}\tau_2^2\mathcal{A}_1 + \frac{9}{2}\mathbf{c}_{11}\mathbb{k}^4\sigma_{11}\tau_1\tau_3\mathcal{A}_1 + 12\mathbf{c}_{11}\mathbb{k}^4\sigma_{11}\tau_0\tau_4\mathcal{A}_1,\\
0 &= \frac{1}{2}\tau_1\mathcal{L}_1\mathcal{A}_1^3 + \tau_1\mathcal{L}_2\mathcal{A}_1^3 + 2\tau_2\mathcal{L}_1\mathcal{A}_0\mathcal{A}_1^2 + \tau_2\mathcal{L}_2\mathcal{A}_0\mathcal{A}_1^2 + \frac{3}{2}\tau_3\mathcal{L}_1\mathcal{A}_0^2\mathcal{A}_1 + \frac{3}{2}\tau_3\mathcal{L}_0\mathcal{A}_1 + \frac{7}{2}\tau_3\mathcal{L}_1\mathcal{A}_1^2\mathcal{B}_1 - \tau_3\mathcal{L}_2\mathcal{A}_1^2\mathcal{B}_1\\
&\quad + 4\tau_4\mathcal{L}_1\mathcal{A}_0\mathcal{A}_1\mathcal{B}_1 - 2\tau_4\mathcal{L}_2\mathcal{A}_0\mathcal{A}_1\mathcal{B}_1 + 20\mathcal{L}_5\mathcal{A}_0\mathcal{A}_1^3\mathcal{B}_1 + 10\mathcal{L}_5\mathcal{A}_0^3\mathcal{A}_1^2 + 3\mathcal{L}_4\mathcal{A}_0\mathcal{A}_1^2 + \frac{15}{2}\mathbf{c}_{11}\mathbb{k}^4\sigma_{11}\tau_2\tau_3\mathcal{A}_1\\
&\quad + 15\mathbf{c}_{11}\mathbb{k}^4\sigma_{11}\tau_1\tau_4\mathcal{A}_1,\\
0 &= \tau_2\mathcal{L}_1\mathcal{A}_1^3 + \tau_2\mathcal{L}_2\mathcal{A}_1^3 + 3\tau_3\mathcal{L}_1\mathcal{A}_0\mathcal{A}_1^2 + \tau_3\mathcal{L}_2\mathcal{A}_0\mathcal{A}_1^2 + 2\tau_4\mathcal{L}_1\mathcal{A}_0^2\mathcal{A}_1 + 2\tau_4\mathcal{L}_0\mathcal{A}_1 + 4\tau_4\mathcal{L}_1\mathcal{A}_1^2\mathcal{B}_1 - \tau_4\mathcal{L}_2\mathcal{A}_1^2\mathcal{B}_1\\
&\quad + 5\mathcal{L}_5\mathcal{A}_1^4\mathcal{B}_1 + 10\mathcal{L}_5\mathcal{A}_0^2\mathcal{A}_1^3 + \mathcal{L}_4\mathcal{A}_1^3 + \frac{15}{2}\mathbf{c}_{11}\mathbb{k}^4\sigma_{11}\tau_3^2\mathcal{A}_1 + 20\mathbf{c}_{11}\mathbb{k}^4\sigma_{11}\tau_2\tau_4\mathcal{A}_1,\\
0 &= \frac{3}{2}\tau_3\mathcal{L}_1\mathcal{A}_1^3 + \tau_3\mathcal{L}_2\mathcal{A}_1^3 + 4\tau_4\mathcal{L}_1\mathcal{A}_0\mathcal{A}_1^2 + \tau_4\mathcal{L}_2\mathcal{A}_0\mathcal{A}_1^2 + 5\mathcal{L}_5\mathcal{A}_0\mathcal{A}_1^4 + 30\mathbf{c}_{11}\mathbb{k}^4\sigma_{11}\tau_3\tau_4\mathcal{A}_1,\\
0 &= 2\tau_4\mathcal{L}_1\mathcal{A}_1^3 + \tau_4\mathcal{L}_2\mathcal{A}_1^3 + \mathcal{L}_5\mathcal{A}_1^5 + 24\mathbf{c}_{11}\mathbb{k}^4\sigma_{11}\tau_4^2\mathcal{A}_1.
\end{aligned}$$

Solving the above equations with the aid of the Wolfram Mathematica program allows us to get the following results, but satisfying the condition that $\mathcal{A}_1$ and $\mathcal{B}_1$ cannot both be zero simultaneously.

Result 1. If $\tau_0 = \tau_1 = \tau_3 = 0$, then we have

$$\mathcal{A}_0 = \mathcal{B}_1 = 0,\ \mathcal{A}_1 = \pm\sqrt{-\frac{\tau_4 \Upsilon + \tau_4\left(2\mathcal{L}_1 + \mathcal{L}_2\right)}{2\mathcal{L}_5}},\ \tau_2 = \frac{-\mathcal{L}_0 \pm \sqrt{\mathcal{L}_0^2 - 4\mathbf{c}_{11}\mathbb{k}^4\sigma_{11}\mathcal{L}_3}}{2\mathbf{c}_{11}\mathbb{k}^4\sigma_{11}},$$

$$\mathcal{L}_4 = \frac{\left(5\tau_4\Upsilon + \tau_4\left(2\mathcal{L}_1 + 7\mathcal{L}_2\right)\right)\sqrt{\mathcal{L}_0^2 - 4\mathbf{c}_{11}\mathbb{k}^4\sigma_{11}\mathcal{L}_3} + 4\mathcal{L}_0\left(\tau_4\Upsilon + \tau_4\left(\mathcal{L}_1 + 2\mathcal{L}_2\right)\right)}{24\mathbf{c}_{11}\mathbb{k}^4\sigma_{11}\tau_4},$$

where $\Upsilon = \sqrt{(2\mathcal{L}_1 + \mathcal{L}_2)^2 - 96\mathbf{c}_{11}\mathbb{k}^4\sigma_{11}\mathcal{L}_5}$ providing that $(2\mathcal{L}_1 + \mathcal{L}_2)^2 \geq 96\mathbf{c}_{11}\mathbb{k}^4\sigma_{11}\mathcal{L}_5$. Therefore, by considering the acquired set, Eqs (2.2) and (2.3) have the following solutions:

1.1. If $\tau_2 > 0,\ \tau_4 < 0$:

$$\Phi_{1.1}(x,t) = \pm\sqrt{\frac{\tau_2\left(2\mathcal{L}_1 + \mathcal{L}_2 + \Upsilon\right)}{2\mathcal{L}_5}}\operatorname{sech}\left[\mathbb{k}\left(x - \frac{t^\alpha}{\alpha}\nu\right)\sqrt{\tau_2}\right]e^{i\left(-\mathcal{K}x + \omega\frac{t^\alpha}{\alpha} + \theta_0\right)}, \tag{4.26}$$

$$\Psi_{1.1}(x,t) = \pm\varsigma\sqrt{\frac{\tau_2\left(2\mathcal{L}_1 + \mathcal{L}_2 + \Upsilon\right)}{2\mathcal{L}_5}}\operatorname{sech}\left[\mathbb{k}\left(x - \frac{t^\alpha}{\alpha}\nu\right)\sqrt{\tau_2}\right]e^{i\left(-\mathcal{K}x + \omega\frac{t^\alpha}{\alpha} + \theta_0\right)}, \tag{4.27}$$

and these denote bright soliton solutions under the condition that $\mathcal{L}_5\left(2\mathcal{L}_1 + \mathcal{L}_2 + \Upsilon\right) > 0$.

1.2. If $\tau_2 < 0,\ \tau_4 > 0$:

$$\Phi_{1.2}(x,t) = \pm\sqrt{\frac{\tau_2\left(2\mathcal{L}_1 + \mathcal{L}_2 + \Upsilon\right)}{2\mathcal{L}_5}}\sec\left[\mathbb{k}\left(x - \frac{t^\alpha}{\alpha}\nu\right)\sqrt{-\tau_2}\right]e^{i\left(-\mathcal{K}x + \omega\frac{t^\alpha}{\alpha} + \theta_0\right)}, \tag{4.28}$$

$$\Psi_{1.2}(x,t) = \pm\varsigma\sqrt{\frac{\tau_2\left(2\mathcal{L}_1 + \mathcal{L}_2 + \Upsilon\right)}{2\mathcal{L}_5}}\sec\left[\mathbb{k}\left(x - \frac{t^\alpha}{\alpha}\nu\right)\sqrt{-\tau_2}\right]e^{i\left(-\mathcal{K}x + \omega\frac{t^\alpha}{\alpha} + \theta_0\right)}, \tag{4.29}$$

and these describe singular periodic solutions when satisfying the constraint $\mathcal{L}_5\left(2\mathcal{L}_1 + \mathcal{L}_2 + \Upsilon\right) < 0$.

1.3. If $\tau_2 = 0,\ \tau_4 > 0$:

$$\Phi_{1.3}(x,t) = \frac{\sqrt{-\frac{2\mathcal{L}_1 + \mathcal{L}_2 + \Upsilon}{2\mathcal{L}_5}}}{\mathbb{k}\left(x - \frac{t^\alpha}{\alpha}\nu\right)}e^{i\left(-\mathcal{K}x + \omega\frac{t^\alpha}{\alpha} + \theta_0\right)}, \tag{4.30}$$

$$\Psi_{1.3}(x,t) = \varsigma\frac{\sqrt{-\frac{2\mathcal{L}_1 + \mathcal{L}_2 + \Upsilon}{2\mathcal{L}_5}}}{\mathbb{k}\left(x - \frac{t^\alpha}{\alpha}\nu\right)}e^{i\left(-\mathcal{K}x + \omega\frac{t^\alpha}{\alpha} + \theta_0\right)}, \tag{4.31}$$

which denote rational solutions such that $\mathcal{L}_5\left(2\mathcal{L}_1 + \mathcal{L}_2 + \Upsilon\right) < 0$.

Result 2. If $\tau_1 = \tau_3 = \mathcal{B}_1 = 0$, then

$$\mathcal{A}_0 = 0,\ \mathcal{A}_1 = \pm\sqrt{-\frac{\tau_4\left(2\mathcal{L}_1+\mathcal{L}_2+\Upsilon\right)}{2\mathcal{L}_5}},\ \tau_2 = \frac{-\mathcal{L}_0 \pm \sqrt{\frac{2\mathbf{c}_{11}\mathbb{k}^4\sigma_{11}\left(\tau_0\left(\tau_4\left(-24\mathbf{c}_{11}\mathbb{k}^4\sigma_{11}\mathcal{L}_5+\mathcal{L}_2^2+2\mathcal{L}_1\mathcal{L}_2\right)+\tau_4\mathcal{L}_2\Upsilon\right)-2\mathcal{L}_3\mathcal{L}_5\right)}{\mathcal{L}_5}+\mathcal{L}_0^2}}{2\mathbf{c}_{11}\mathbb{k}^4\sigma_{11}},$$

$$\mathcal{L}_4 = \frac{\left(5\tau_4\Upsilon+\tau_4\left(2\mathcal{L}_1+7\mathcal{L}_2\right)\right)\sqrt{\mathcal{L}_0^2-\frac{2\mathbf{c}_{11}\mathbb{k}^4\sigma_{11}\left(\tau_0\left(\tau_4(-\mathcal{L}_2)\Upsilon-\tau_4\left(-24\mathbf{c}_{11}\mathbb{k}^4\sigma_{11}\mathcal{L}_5+\mathcal{L}_2^2+2\mathcal{L}_1\mathcal{L}_2\right)\right)+2\mathcal{L}_3\mathcal{L}_5\right)}{\mathcal{L}_5}}+4\mathcal{L}_0\left(\tau_4\Upsilon+\tau_4\left(\mathcal{L}_1+2\mathcal{L}_2\right)\right)}{24\mathbf{c}_{11}\mathbb{k}^4\sigma_{11}\tau_4},$$

where $\Upsilon = \sqrt{(2\mathcal{L}_1+\mathcal{L}_2)^2-96\mathbf{c}_{11}\mathbb{k}^4\sigma_{11}\mathcal{L}_5}$, providing that $(2\mathcal{L}_1+\mathcal{L}_2)^2 \geq 96\mathbf{c}_{11}\mathbb{k}^4\sigma_{11}\mathcal{L}_5$. Therefore, when considering the acquired set of solutions, Eqs (2.2) and (2.3) have the following solutions:

2.1. If $\tau_2 < 0,\ \tau_4 > 0$, and $\tau_0 = \frac{\tau_2^2}{4\tau_4}$, then

$$\Phi_{2.1}(x,t) = \frac{1}{2}\sqrt{\frac{\tau_2\left(2\mathcal{L}_1+\mathcal{L}_2+\Upsilon\right)}{\mathcal{L}_5}}\tanh\left[\mathbb{k}\left(x-\nu\frac{t^\alpha}{\alpha}\right)\sqrt{-\frac{\tau_2}{2}}\right]e^{i\left(-\mathcal{K}x+\omega\frac{t^\alpha}{\alpha}+\theta_0\right)}, \tag{4.32}$$

$$\Psi_{2.1}(x,t) = \frac{\varsigma}{2}\sqrt{\frac{\tau_2\left(2\mathcal{L}_1+\mathcal{L}_2+\Upsilon\right)}{\mathcal{L}_5}}\tanh\left[\mathbb{k}\left(x-\nu\frac{t^\alpha}{\alpha}\right)\sqrt{-\frac{\tau_2}{2}}\right]e^{i\left(-\mathcal{K}x+\omega\frac{t^\alpha}{\alpha}+\theta_0\right)}, \tag{4.33}$$

and these are considered as dark soliton solutions such that $\mathcal{L}_5\left(2\mathcal{L}_1+\mathcal{L}_2+\Upsilon\right) < 0$.

2.2. If $\tau_2 > 0,\ \tau_4 > 0$, and $\tau_0 = \frac{\tau_2^2}{4\tau_4}$, then

$$\Phi_{2.2}(x,t) = \frac{1}{2}\sqrt{\frac{\tau_2\left(2\mathcal{L}_1+\mathcal{L}_2+\Upsilon\right)}{\mathcal{L}_5}}\tan\left[\mathbb{k}\left(x-\nu\frac{t^\alpha}{\alpha}\right)\sqrt{\frac{\tau_2}{2}}\right]e^{i\left(-\mathcal{K}x+\omega\frac{t^\alpha}{\alpha}+\theta_0\right)}, \tag{4.34}$$

$$\Psi_{2.2}(x,t) = \frac{\varsigma}{2}\sqrt{\frac{\tau_2\left(2\mathcal{L}_1+\mathcal{L}_2+\Upsilon\right)}{\mathcal{L}_5}}\tan\left[\mathbb{k}\left(x-\nu\frac{t^\alpha}{\alpha}\right)\sqrt{\frac{\tau_2}{2}}\right]e^{i\left(-\mathcal{K}x+\omega\frac{t^\alpha}{\alpha}+\theta_0\right)}, \tag{4.35}$$

and these are singular periodic solutions such that $\mathcal{L}_5\left(2\mathcal{L}_1+\mathcal{L}_2+\Upsilon\right) > 0$.

2.3. If $\tau_2 > 0,\ \tau_4 < 0,\ \tau_0 = \frac{m^2\left(1-m^2\right)\tau_2^2}{\left(2m^2-1\right)^2\tau_4}$, and $0 < m \leq 1$, Jacobi elliptic function (JEF) solutions are given provided that $m \neq \dfrac{1}{\sqrt{2}}$ and $\mathcal{L}_5\left(\mathcal{L}_2\Upsilon+2\mathcal{L}_1\right) > 0$:

$$\Phi_{2.3}(x,t) = \pm m\sqrt{-\frac{\tau_2\left(\mathcal{L}_2\Upsilon+2\mathcal{L}_1\right)}{2\left(1-2m^2\right)\mathcal{L}_5}}\ \mathrm{cn}\left[\mathbb{k}\left(x-\nu\frac{t^\alpha}{\alpha}\right)\right]e^{i\left(-\mathcal{K}x+\omega\frac{t^\alpha}{\alpha}+\theta_0\right)}, \tag{4.36}$$

$$\Psi_{2.3}(x,t) = \pm m\,\varsigma\sqrt{-\frac{\tau_2\left(\mathcal{L}_2\Upsilon+2\mathcal{L}_1\right)}{2\left(1-2m^2\right)\mathcal{L}_5}}\ \mathrm{cn}\left[\mathbb{k}\left(x-\nu\frac{t^\alpha}{\alpha}\right)\right]e^{i\left(-\mathcal{K}x+\omega\frac{t^\alpha}{\alpha}+\theta_0\right)}. \tag{4.37}$$

2.4. If $\tau_2 > 0,\ \tau_4 < 0,\ \tau_0 = \frac{\left(1-m^2\right)\tau_2^2}{\left(2-m^2\right)^2\tau_4},\ \mathcal{L}_5\left(2\mathcal{L}_1+\mathcal{L}_2+\Upsilon\right) > 0$, and $0 < m \leq 1$, JEF solutions are constructed as

$$\Phi_{2.4}(x,t) = \pm m\sqrt{\frac{2\mathcal{L}_1+\mathcal{L}_2+\Upsilon}{2\left(2-m^2\right)\mathcal{L}_5}}\ \mathrm{dn}\left[\mathbb{k}\left(x-\nu\frac{t^\alpha}{\alpha}\right)\right]e^{i\left(-\mathcal{K}x+\omega\frac{t^\alpha}{\alpha}+\theta_0\right)}, \tag{4.38}$$

$$\Psi_{2.4}(x,t) = \pm m\,\varsigma\sqrt{\frac{2\mathcal{L}_1+\mathcal{L}_2+\Upsilon}{2\left(2-m^2\right)\mathcal{L}_5}}\,\mathrm{dn}\left[\mathbb{k}\left(x-\nu\frac{t^{\alpha}}{\alpha}\right)\right]e^{i\left(-\mathcal{K}x+\omega\frac{t^{\alpha}}{\alpha}+\theta_0\right)}, \tag{4.39}$$

and when setting $m=1$, bright soliton solutions can be given as

$$\Phi_{2.5}(x,t) = \pm\sqrt{\frac{2\mathcal{L}_1+\mathcal{L}_2+\Upsilon}{2\mathcal{L}_5}}\mathrm{sech}\left[\mathbb{k}\left(x-\nu\frac{t^{\alpha}}{\alpha}\right)\right]e^{i\left(-\mathcal{K}x+\omega\frac{t^{\alpha}}{\alpha}+\theta_0\right)}, \tag{4.40}$$

$$\Psi_{2.5}(x,t) = \pm\varsigma\sqrt{\frac{2\mathcal{L}_1+\mathcal{L}_2+\Upsilon}{2\mathcal{L}_5}}\mathrm{sech}\left[\mathbb{k}\left(x-\nu\frac{t^{\alpha}}{\alpha}\right)\right]e^{i\left(-\mathcal{K}x+\omega\frac{t^{\alpha}}{\alpha}+\theta_0\right)}. \tag{4.41}$$

2.5. If $\tau_2<0,\ \tau_4>0,\ \tau_0=\frac{m^2\tau_2^2}{\left(1+m^2\right)^2\tau_4},\ \mathcal{L}_5\left(2\mathcal{L}_1+\mathcal{L}_2+\Upsilon\right)<0$, and $0<m\le 1$, JEF solutions are given as

$$\Phi_{2.6}(x,t) = m\sqrt{\frac{\tau_2\left(2\mathcal{L}_1+\mathcal{L}_2+\Upsilon\right)}{2\left(m^2+1\right)\mathcal{L}_5}}\,\mathrm{sn}\left[\mathbb{k}\left(x-\nu\frac{t^{\alpha}}{\alpha}\right)\right]e^{i\left(-\mathcal{K}x+\omega\frac{t^{\alpha}}{\alpha}+\theta_0\right)}, \tag{4.42}$$

$$\Psi_{2.6}(x,t) = m\,\varsigma\sqrt{\frac{\tau_2\left(2\mathcal{L}_1+\mathcal{L}_2+\Upsilon\right)}{2\left(m^2+1\right)\mathcal{L}_5}}\,\mathrm{sn}\left[\mathbb{k}\left(x-\nu\frac{t^{\alpha}}{\alpha}\right)\right]e^{i\left(-\mathcal{K}x+\omega\frac{t^{\alpha}}{\alpha}+\theta_0\right)}. \tag{4.43}$$

Result 3. If $\tau_3=\tau_4=0$, and $\Upsilon=\sqrt{\left(2\mathcal{L}_1+\mathcal{L}_2\right)^2-96\mathbf{c}_{11}\mathbb{k}^4\sigma_{11}\mathcal{L}_5}$ such that $\left(2\mathcal{L}_1+\mathcal{L}_2\right)^2\ge 96\mathbf{c}_{11}\mathbb{k}^4\sigma_{11}\mathcal{L}_5$, then, in this case, we find:

3.1. $\mathcal{A}_1=0,\ \mathcal{A}_0=\pm\frac{1}{2}\sqrt{-\frac{\tau_2\left(2\mathcal{L}_1+\mathcal{L}_2+\Upsilon\right)}{2\mathcal{L}_5}},\ \mathcal{B}_1=\pm\frac{\tau_1}{2}\sqrt{-\frac{2\mathcal{L}_1+\mathcal{L}_2+\Upsilon}{2\tau_2\mathcal{L}_5}},\ \tau_0=\frac{\tau_1^2}{4\tau_2}$,

$$\mathcal{L}_0=\frac{\tau_2\left(-\left(-32\mathbf{c}_{11}\mathbb{k}^4\sigma_{11}\mathcal{L}_5+\mathcal{L}_2^2+2\mathcal{L}_1\mathcal{L}_2\right)\right)\pm\tau_2\mathcal{L}_2\Upsilon}{16\mathcal{L}_5}+\frac{2\mathcal{L}_3}{\tau_2},$$

$$\mathcal{L}_4=\frac{\Upsilon\left(3\mathbf{c}_{11}\mathbb{k}^4\sigma_{11}\tau_2^2-2\mathcal{L}_3\right)+2\mathcal{L}_1\left(3\mathbf{c}_{11}\mathbb{k}^4\sigma_{11}\tau_2^2+2\mathcal{L}_3\right)+\mathcal{L}_2\left(3\mathbf{c}_{11}\mathbb{k}^4\sigma_{11}\tau_2^2+2\mathcal{L}_3\right)}{24\mathbf{c}_{11}\mathbb{k}^4\sigma_{11}\tau_2}.$$

3.2. $\mathcal{A}_0=\mathcal{A}_1=\tau_1=0,\ \mathcal{B}_1=\pm\sqrt{-\frac{\tau_0\left(2\mathcal{L}_1+\mathcal{L}_2+\Upsilon\right)}{2\mathcal{L}_5}},\ \mathcal{L}_0=-\frac{\mathbf{c}_{11}\mathbb{k}^4\sigma_{11}\tau_2^2+\mathcal{L}_3}{\tau_2}$,

$$\mathcal{L}_4=\frac{\Upsilon\left(\mathcal{L}_3-9\mathbf{c}_{11}\mathbb{k}^4\sigma_{11}\tau_2^2\right)-2\mathcal{L}_1\left(3\mathbf{c}_{11}\mathbb{k}^4\sigma_{11}\tau_2^2+\mathcal{L}_3\right)-\mathcal{L}_2\left(15\mathbf{c}_{11}\mathbb{k}^4\sigma_{11}\tau_2^2+\mathcal{L}_3\right)}{24\mathbf{c}_{11}\mathbb{k}^4\sigma_{11}\tau_2}.$$

From the set (3.1), we may build the next exponential solutions as follows:

$$\Phi_{3.1}(x,t) = \pm\frac{1}{2}\left(\frac{\sqrt{2}\tau_1\tau_2\sqrt{-\frac{2\mathcal{L}_1+\mathcal{L}_2+\Upsilon}{\tau_2\mathcal{L}_5}}}{2\tau_2 e^{\mathbb{k}\sqrt{\tau_2}\left(x-\frac{\nu t^{\alpha}}{\alpha}\right)}-\tau_1}+\sqrt{-\frac{\tau_2\left(2\mathcal{L}_1+\mathcal{L}_2+\Upsilon\right)}{2\mathcal{L}_5}}\right)e^{i\left(-\mathcal{K}x+\omega\frac{t^{\alpha}}{\alpha}+\theta_0\right)}, \tag{4.44}$$

$$\Psi_{3.1}(x,t) = \pm\frac{\varsigma}{2}\left(\frac{\sqrt{2}\tau_1\tau_2\sqrt{-\frac{2\mathcal{L}_1+\mathcal{L}_2+\Upsilon}{\tau_2\mathcal{L}_5}}}{2\tau_2 e^{\mathbb{k}\sqrt{\tau_2}\left(x-\frac{\nu t^{\alpha}}{\alpha}\right)}-\tau_1}+\sqrt{-\frac{\tau_2\left(2\mathcal{L}_1+\mathcal{L}_2+\Upsilon\right)}{2\mathcal{L}_5}}\right)e^{i\left(-\mathcal{K}x+\omega\frac{t^{\alpha}}{\alpha}+\theta_0\right)}, \tag{4.45}$$

provided that $\tau_2 > 0$, $\mathcal{L}_5\left(2\mathcal{L}_1 + \mathcal{L}_2 + \Upsilon\right) < 0$, and $2\tau_2 e^{\Bbbk\sqrt{\tau_2}\left(x-\frac{\nu t^\alpha}{\alpha}\right)} - \tau_1 \neq 0$.
From the set (3.2), we can construct the following solutions such that $\mathcal{L}_5\left(2\mathcal{L}_1 + \mathcal{L}_2 + \Upsilon\right) < 0$:

3.2.1. If $\tau_0 > 0$ and $\tau_2 < 0$, singular periodic solutions are obtained:

$$\Phi_{3.2,1}(x,t) = \pm\sqrt{\frac{\tau_2\left(2\mathcal{L}_1 + \mathcal{L}_2 + \Upsilon\right)}{2\mathcal{L}_5}}\csc\left[\Bbbk\left(x - \nu\frac{t^\alpha}{\alpha}\right)\sqrt{-\tau_2}\right]e^{i\left(-\mathcal{K}x+\omega\frac{t^\alpha}{\alpha}+\theta_0\right)}, \tag{4.46}$$

$$\Psi_{3.2,1}(x,t) = \pm\varsigma\sqrt{\frac{\tau_2\left(2\mathcal{L}_1 + \mathcal{L}_2 + \Upsilon\right)}{2\mathcal{L}_5}}\csc\left[\Bbbk\left(x - \nu\frac{t^\alpha}{\alpha}\right)\sqrt{-\tau_2}\right]e^{i\left(-\mathcal{K}x+\omega\frac{t^\alpha}{\alpha}+\theta_0\right)}. \tag{4.47}$$

3.2.2. If $\tau_0 > 0$ and $\tau_2 > 0$, singular soliton solutions are found:

$$\Phi_{3.2,2}(x,t) = \pm\sqrt{-\frac{\tau_2\left(2\mathcal{L}_1 + \mathcal{L}_2 + \Upsilon\right)}{2\mathcal{L}_5}}\operatorname{csch}\left[\Bbbk\left(x - \nu\frac{t^\alpha}{\alpha}\right)\sqrt{\tau_2}\right]e^{i\left(-\mathcal{K}x+\omega\frac{t^\alpha}{\alpha}+\theta_0\right)}, \tag{4.48}$$

$$\Psi_{3.2,2}(x,t) = \pm\varsigma\sqrt{-\frac{\tau_2\left(2\mathcal{L}_1 + \mathcal{L}_2 + \Upsilon\right)}{2\mathcal{L}_5}}\operatorname{csch}\left[\Bbbk\left(x - \nu\frac{t^\alpha}{\alpha}\right)\sqrt{\tau_2}\right]e^{i\left(-\mathcal{K}x+\omega\frac{t^\alpha}{\alpha}+\theta_0\right)}. \tag{4.49}$$

5. Conformable fractional derivative influence on the extracted solutions

By altering the model's parameter values, several categories of solutions for Eqs (2.2) and (2.3) might be extracted. Consequently, this technique has yielded a set of remarkable results that, to the best of our knowledge, have not been previously reported or achieved in the existing literature. The two- and three-dimensional simulation generated sketches of a number of specific solutions that demonstrate the physical characteristics of the retrieved solutions (see Table 1). These graphical simulations will show how robust the higher solutions are against perturbations, and they are made using the Wolfram Mathematica software.

Figure 1 shows the 3D plots of Eq (4.26) by using different conformable fractional derivative parameters aligned with the collective 2D plots for all cases. These bright solitons are linked to localized wave packets that maintain their shape and energy for long distances, commonly occurring in optical fibers and plasma channels. In addition, Figure 2 displays the same plots but for Eq (4.27) using the same values in Figure 1.

Figure 3 displays the 3D plots of Eq (4.30) by using different fractional order α aligned with the collective 2D plots for all cases. In addition, Figure 4 displays the same plots but for Eq (4.31) using the same values in Figure 3. These rational solutions, typically expressed in the form of ratios of polynomials, have been found to be related to rogue wave or wave amplification phenomena in nonlinear media. They are spatially and temporally localized and often used to model extreme wave phenomena in optical fibers, deep ocean waves, and plasma systems. Their analytical character allows the modeling of high-amplitude transient behavior far from normal wave behavior, which gives insights into wave focusing and instabilities in complicated systems.

In Figure 5, we showed the 3D plots of Eq (4.32) by using different fractional-order α aligned with the collective 2D plots for all cases. These dark solitons are localized depressions of a long-lived wave background, of interest in signal void description in nonlinear optics and Bose-Einstein condensates. In addition, Figure 6 displays the same plots but for Eq (4.33) using the same values in Figure 5.

Figures 7 and 8 display the solution of Eqs (4.34) and (4.35), respectively. The singular soliton solutions in Eqs (4.46) and (4.47) are represented in Figures 9 and 10. Singular solitons and singular periodic solutions commonly indicate wave localization or blow-up behavior and represent important transitions in highly nonlinear regimes. The plots in Figure 11, clearly show the effect of the fractional-order parameter α on the displacement $x(t)$ and the velocity $v(t)$ of the wave packet or pulse with respect to time. In the left plot, the trajectories of the position with respect to time for different α values show that the pulse is not travelling in a straight line; rather, its movement slows or accelerates depending on the fractional order. Particularly for smaller α ($\alpha = 0.4$), the displacement curve starts rapidly but slows down in the latter half, while larger α values ($\alpha = 0.9$) are associated with faster, almost linear propagation.

In the right plot, the profiles of velocity demonstrate that there's an initial drastic reduction, especially in the case of small α, indicating that fractional derivatives produce memory effects that delay the system after a burst. The velocity stabilizes sooner as α increases. All these results confirm that fractional-order time derivatives cause non-local temporal behavior that alters both speed and path of the pulse compared to classical models.

Table 1. Summary of the values of all plots.

Figure number	Type of the solution	Parameters' values	x–domain
Figures 1 and 2	bright soliton	$\mathcal{K} = 0.6$, $\mathbf{a}_1 = 0.7$, $\mathbf{c}_{21} = 0.5$, $\Bbbk = 0.5$, $\mathbf{c}_{11} = 0.65$, $\delta_1 = 0.9$, $\mu_1 = 0.8$, $\varsigma = 1.5$, $\zeta_1 = 0.65$, $\rho_1 = 0.8$, $\mathcal{A}_1 = 0.85$, $\gamma_1 = 1.5$, $\mathcal{B}_1 = 0.85$, $\lambda_1 = 0.9$, $\sigma_{11} = 0.6$, $\sigma_{71} = 0.8$, $\omega = 0.5$, $\theta_0 = 0.8$, $\mathbf{f}_1 = 0.5$, $\mathbf{g}_1 = 0.6$, $\mathbf{h}_1 = 0.5$	$-15 \le x \le 15$
Figures 3 and 4	rational	$\mathcal{K} = 0.5$, $\mathbf{a}_1 = 0.8$, $\mathbf{c}_{21} = 0.6$, $\Bbbk = 0.7$, $\mathbf{c}_{11} = 0.75$, $\delta_1 = 0.8$, $\mu_1 = 0.9$, $\varsigma = 2$, $\zeta_1 = 0.6$, $\rho_1 = 0.9$, $\mathcal{A}_1 = 1.5$, $\gamma_1 = 1.3$, $\mathcal{B}_1 = 1.8$, $\lambda_1 = 1.9$, $\sigma_{11} = 0.7$, $\sigma_{71} = 0.8$, $\omega = 0.75$, $\theta_0 = 0.85$, $\mathbf{f}_1 = -1.55$, $\mathbf{g}_1 = 0.65$, $\mathbf{h}_1 = -0.75$	$-15 \le x \le 15$
Figures 5 and 6	dark soliton	$\mathcal{K} = 0.7$, $\mathbf{a}_1 = 0.8$, $\mathbf{c}_{21} = 0.6$, $\Bbbk = 0.7$, $\mathbf{c}_{11} = -0.5$, $\delta_1 = 0.8$, $\mu_1 = 0.85$, $\varsigma = 2.5$, $\zeta_1 = 0.6$, $\rho_1 = 0.7$, $\mathcal{A}_1 = 0.8$, $\gamma_1 = 1.4$, $\mathcal{B}_1 = 0.95$, $\lambda_1 = 0.8$, $\sigma_{11} = -0.4$, $\sigma_{71} = 0.85$, $\omega = 0.6$, $\theta_0 = 0.9$, $\mathbf{f}_1 = 0.6$, $\mathbf{g}_1 = 0.5$, $\mathbf{h}_1 = 0.6$, $\tau_0 = 0.7$, $\tau_4 = 0.6$	$-15 \le x \le 15$
Figures 7 and 8	singular periodic	$\mathcal{K} = 0.6$, $\mathbf{a}_1 = 0.9$, $\mathbf{c}_{21} = 0.75$, $\Bbbk = 0.8$, $\mathbf{c}_{11} = 0.6$, $\delta_1 = 0.9$, $\mu_1 = 0.95$, $\varsigma = 2$, $\zeta_1 = 0.7$, $\rho_1 = 0.75$, $\mathcal{A}_1 = 0.85$, $\gamma_1 = 1.5$, $\mathcal{B}_1 = 0.85$, $\lambda_1 = 0.7$, $\sigma_{11} = -0.6$, $\sigma_{71} = 0.95$, $\omega = 0.7$, $\theta_0 = 0.8$, $\mathbf{f}_1 = 0.7$, $\mathbf{g}_1 = 0.6$, $\mathbf{h}_1 = 0.8$, $\tau_0 = 0.7$, $\tau_4 = 0.6$	$-5 \le x \le 5$
Figures 9 and 10	singular soliton	$\mathcal{K} = 0.9$, $\mathbf{a}_1 = 0.6$, $\mathbf{c}_{21} = 0.9$, $\Bbbk = -0.6$, $\mathbf{c}_{11} = -0.5$, $\delta_1 = 0.8$, $\mu_1 = 0.9$, $\varsigma = 2$, $\zeta_1 = 0.65$, $\rho_1 = 0.8$, $\mathcal{A}_1 = 0.85$, $\gamma_1 = 1.5$, $\mathcal{B}_1 = 0.95$, $\lambda_1 = 1$, $\sigma_{11} = -0.7$, $\sigma_{71} = 0.85$, $\omega = 0.7$, $\theta_0 = 0.9$, $\mathbf{f}_1 = 0.7$, $\mathbf{g}_1 = 0.8$, $\mathbf{h}_1 = 1.9$, $\tau_2 = 0.8$	$-15 \le x \le 15$
Figures 11	position and velocity profiles	$\alpha_1 = 0.4$, $\alpha_2 = 0.7$, $\alpha_3 = 0.9$, $\mathcal{K} = -0.5$, $\mathbf{a}_1 = 0.8$, $\mathbf{c}_{21} = 0.7$, $\sigma_{71} = 0.85$	– – –

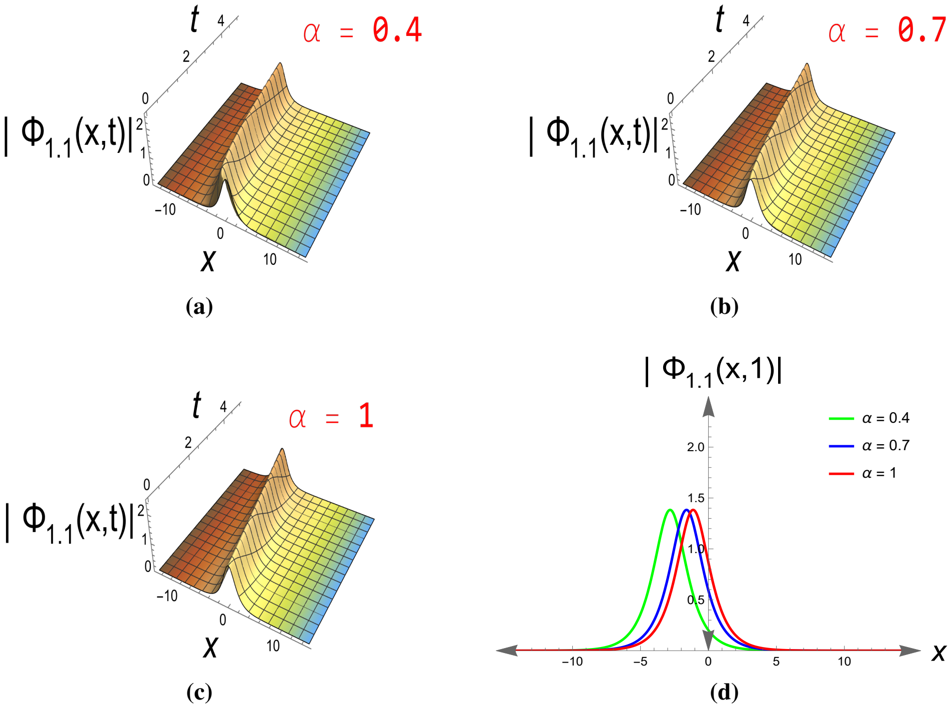

Figure 1. Graphical depictions of the bright soliton solution of Eq (4.26).

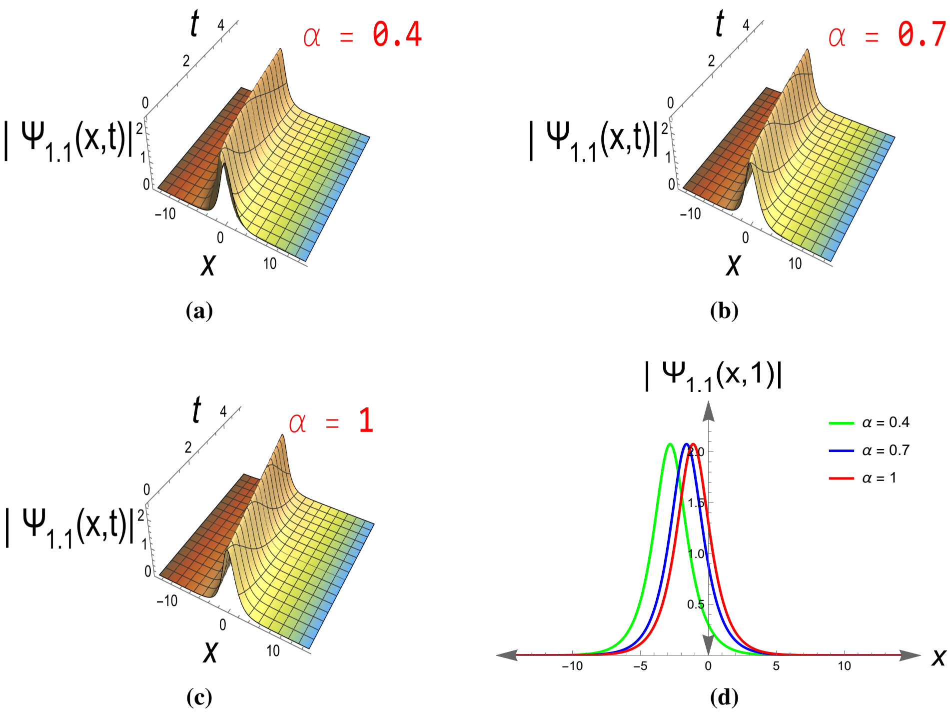

Figure 2. Graphical depictions of the bright soliton solution of Eq (4.27).

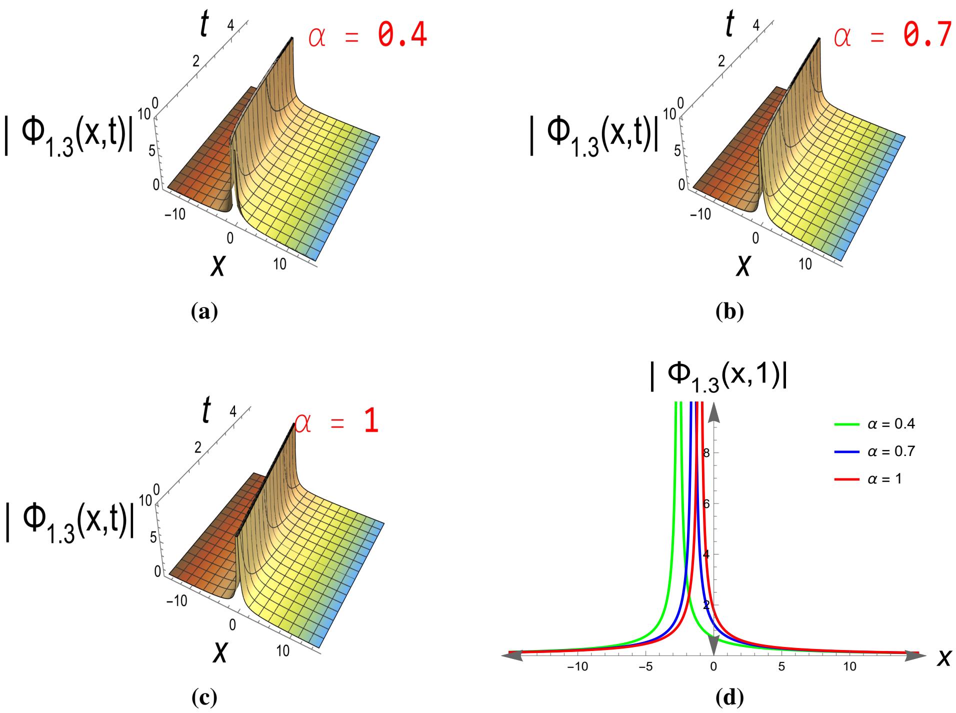

Figure 3. Graphical depictions of the rational solution of Eq (4.30).

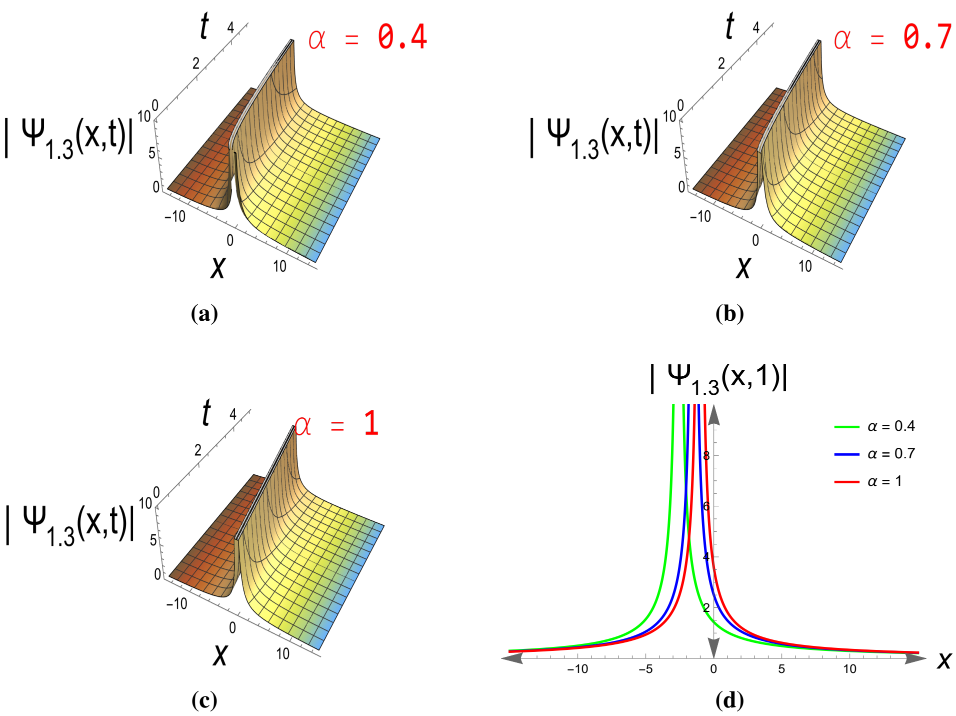

Figure 4. Graphical depictions of the rational solution of Eq (4.31).

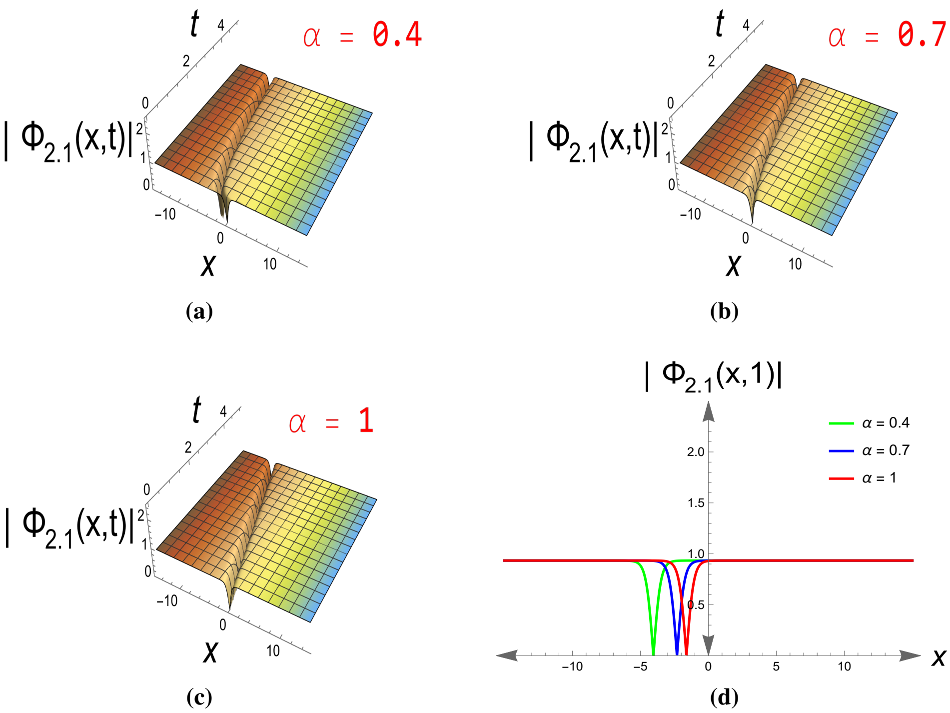

Figure 5. Graphical depictions of the dark soliton solution of Eq (4.32).

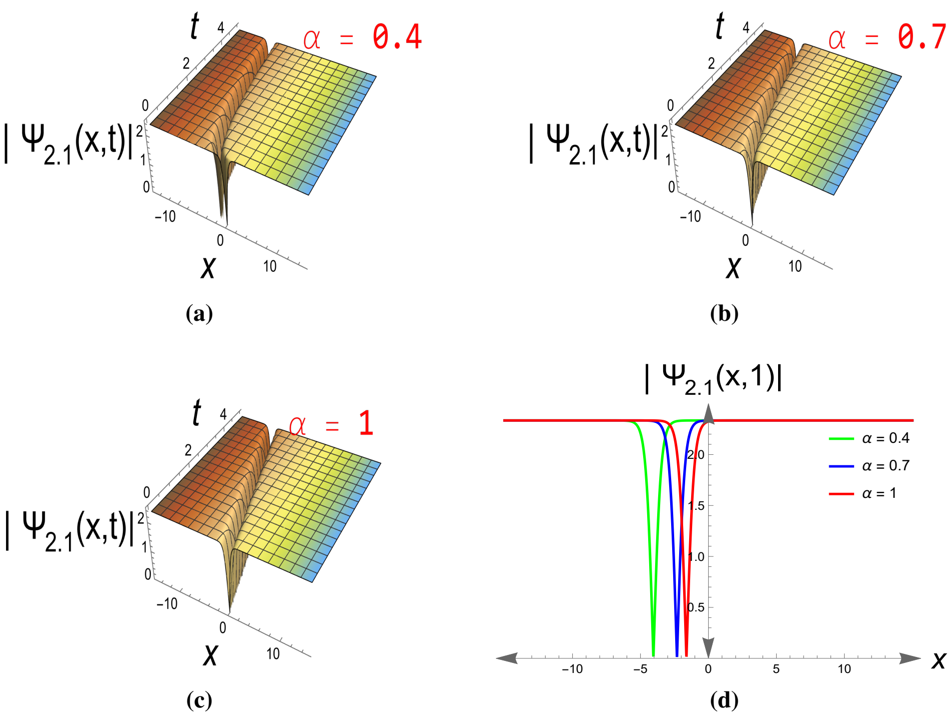

Figure 6. Graphical depictions of the dark soliton solution of Eq (4.33).

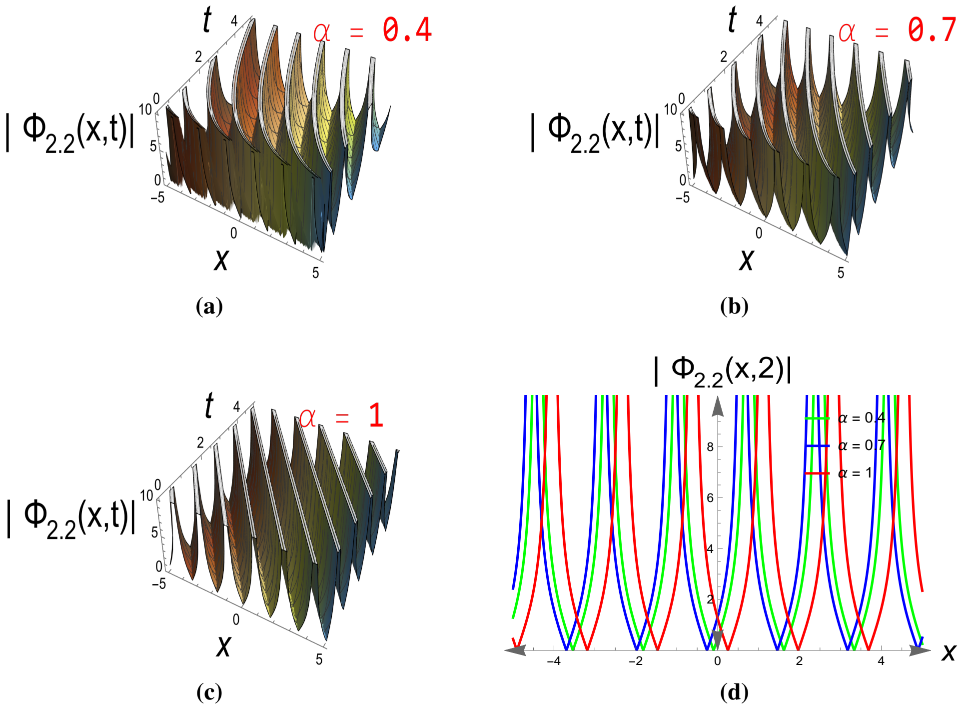

Figure 7. Graphical depictions of the singular periodic solution of Eq (4.34).

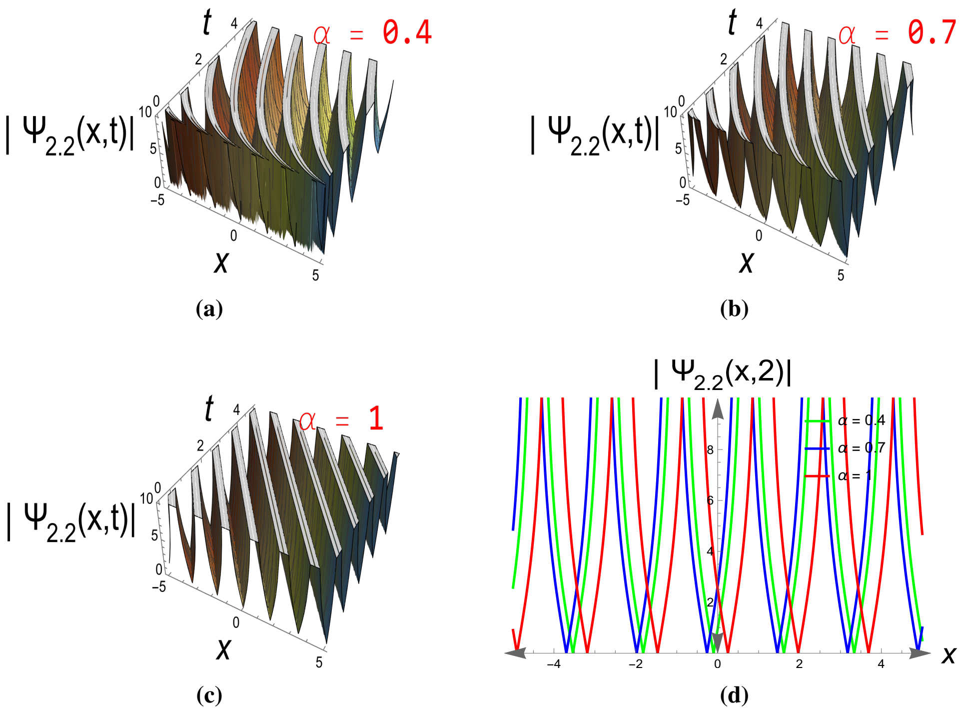

Figure 8. Graphical depictions of the singular periodic solution of Eq (4.35).

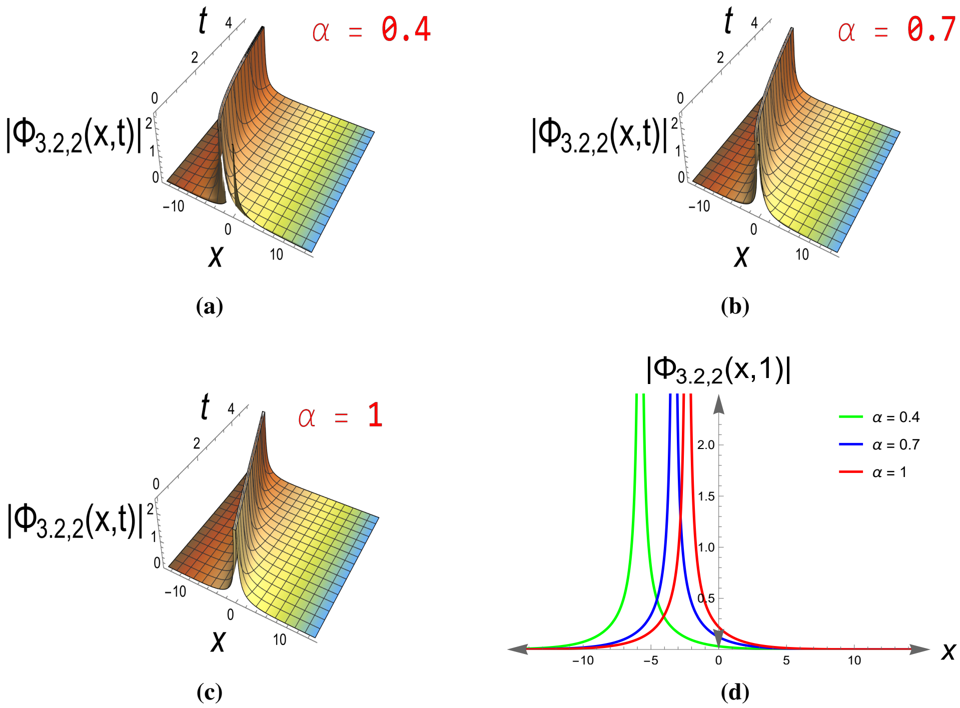

Figure 9. Graphical depictions of the singular soliton solution of Eq (4.46).

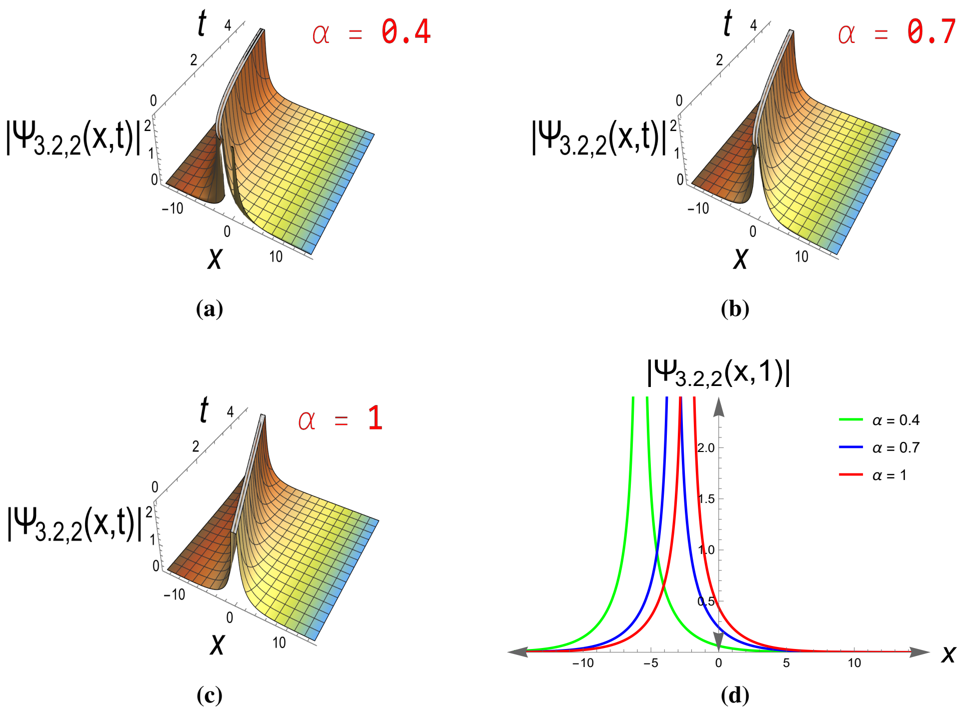

Figure 10. Graphical depictions of the singular soliton solution of Eq (4.47).

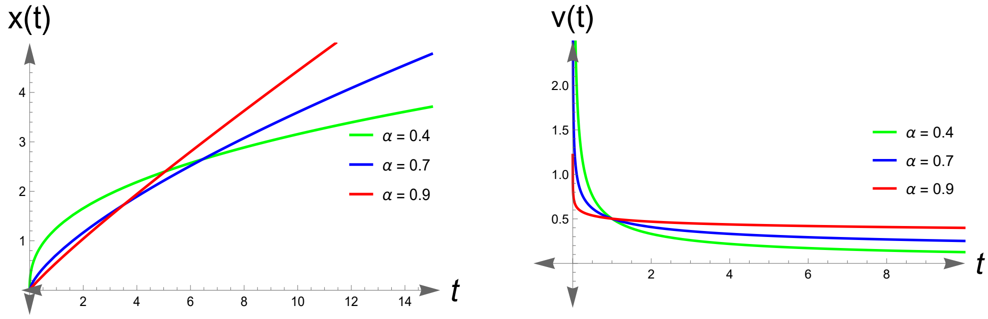

(a) position profile

(b) velocity profile

Figure 11. Graphical depictions of the influence of fractional derivative parameter on position and velocity profiles.

6. Comparison with literature

While previous efforts, such as [37], considered the concatenation model in birefringent fibers using classical methods like the enhanced Kudryashov method and unveiled diverse solution families like kink-type, rational, and shock structures, the current work extends this framework by invoking conformable fractional derivatives. In contrast to integer-order models, the inclusion of the fractional-order operator provides hereditary and memory effects in optical fiber media necessary for pulse evolution modeling in nonlinear dispersive media with complex response properties. The conformable derivative is of specific interest due to its compatibility with conventional chain rules and simpler numerical implementation compared to Riemann–Liouville or Caputo versions. This extension allows for more intricate wave structures and parameter sensitivity, a more flexible framework with which to model temporal dispersion and nonlocality in birefringent optical fibers, the latter of which is important in modern photonic communication systems. A comparison, side by side, of our fractional-based solutions and those obtained by Ekici and Sarmaşık [37] highlights new dynamical behaviors, especially under variation of the fractional order, that are evasive to classical models. Also, the model discussed in [38] only applied the stochastic perturbation of some analytical solutions for the concatenation model with spatio-temporal dispersion having multiplicative white noise.

7. Conclusions

The concatenation-type governing equation of optical solitons in a birefringent fiber, including conformable fractional derivatives, was studied in this paper. To create the model, three conventional equations are concatenated. They are the LPD model, the SSE, and the most well-known NLSE. Using the principle of the IME tanh function algorithm, the research model was integrated. The model's bright, dark, and singular solitons were therefore recovered, together with the relevant constraint conditions that arose organically during the soliton solution's derivation. The technique used yields a large number of solutions that are unique, such as JEFs, exponential, rational, and singular periodic solutions. Our article has the greatest number of solutions when compared with what exists in the literature.

Future research might focus on examining the stability and long-term characteristics of the discovered solitary wave solutions. Investigating parametric changes and their effects on the system dynamics may reveal more intriguing events. Combining analytical and numerical approaches might lead to a deeper understanding of this complex subject. In conclusion, this text's results persuasively demonstrate how effective and potent the IME tanh function technique mentioned above is at precisely solving NLPDEs both now and in the future.

Author contributions

Altaf Alshuhail: Methodology, software; Hamdy M. Ahmed: Formal analysis, investigation; Abeer S. Khalifa: Software, writing-original draft, writing-review & editing; Wael W. Mohammed: Data curation, resources, supervision; Mohamed S Algolam: Investigation, writing-original draft, visualization; Athar I Ahmed: Investigation, resources; Karim K. Ahmed: Data curation, validation, writing-original draft. All authors have read and approved the final version of the manuscript for publication.

Use of Generative-AI tools declaration

The authors declare that they have not used Artificial Intelligence tools in the creation of this article.

Acknowledgments

This research has been funded by Scientific Research Deanship at the University of Ha'il-Saudi Arabia through project number RG-25005.

Conflict of interest

All authors declare no conflicts of interest in this paper.

References

1. B. Guo, L. Ling, Q. P. Liu, Nonlinear Schrödinger equation: Generalized Darboux transformation and rogue wave solutions, *Phys. Rev. E*, **85** (2012), 026607. https://doi.org/10.1103/PhysRevE.85.026607
2. D. W. Zuo, Y. T. Gao, L. Xue, Y. J. Feng, Lax pair, roguewave and soliton solutions for a variable-coefficient generalized nonlinear Schrödinger equation in an optical fiber, fluid or plasma, *Opt. Quant. Electron.*, **48** (2016), 1–4. https://doi.org/10.1007/s11082-015-0290-3
3. N. A. Kudryashov, Embedded solitons of the generalized nonlinear Schrödinger equation with high dispersion, *Regul. Chaotic Dyn.*, **27** (2022), 680–696. https://doi.org/10.1134/S1560354722060065
4. N. H. Ali, S. A. Mohammed, J. Manafian, Study on the simplified MCH equation and the combined KdV-mKdV equations with solitary wave solutions, *Part. Differ. Equ. Appl. Math.*, **9** (2024), 100599. https://doi.org/10.1016/j.padiff.2023.100599

5. K. K. Ahmed, N. M. Badra, H. M. Ahmed, W. B. Rabie, Unveiling optical solitons and other solutions for fourth-order (2+1)-dimensional nonlinear Schrödinger equation by modified extended direct algebraic method, *J. Optics*, 2024, 1–13. https://doi.org/10.1007/s12596-024-01690-8
6. T. Y. Wang, Q. Zhou, W. J. Liu, Soliton fusion and fission for the high-order coupled nonlinear Schrödinger system in fiber lasers, *Chinese Phys. B*, **31** (2022), 020501. https://doi.org/10.1088/1674-1056/ac2d22
7. S. Kumar, N. Mann, Abundant closed-form solutions of the (3+1)-dimensional Vakhnenko-Parkes equation describing the dynamics of various solitary waves in ocean engineering, *J. Ocean Eng. Sci.*, **17** (2022). https://doi.org/10.1016/j.joes.2022.04.007
8. K. K. Ahmed, H. M. Ahmed, N. M. Badra, W. B. Rabie, Optical solitons retrieval for an extension of novel dual-mode of a dispersive non-linear Schrödinger equation, *Optik*, **307** (2024), 171835. https://doi.org/10.1016/j.ijleo.2024.171835
9. Q. Zhou, Y. Sun, H. Triki, Y. Zhong, Z. Zeng, M. Mirzazadeh, Study on propagation properties of one-soliton in a multimode fiber with higher-order effects, *Results Phys.*, **41** (2022), 105898. https://doi.org/10.1016/j.rinp.2022.105898
10. K. K. Ahmed, N. M. Badra, H. M. Ahmed, W. B. Rabie, M. Mirzazadeh, M. Eslami, et al., Investigation of solitons in magneto-optic waveguides with Kudryashov's law nonlinear refractive index for coupled system of generalized nonlinear Schrödinger's equations using modified extended mapping method, *Nonlinear Anal.-Model.*, **29** (2024), 205–223. https://doi.org/10.15388/namc.2024.29.34070
11. A. S. Khalifa, H. M. Ahmed, N. M. Badra, W. B. Rabie, Exploring solitons in optical twin-core couplers with Kerr law of nonlinear refractive index using the modified extended direct algebraic method, *Opt. Quant. Electron.*, **56** (2024), 1060. https://doi.org/10.1007/s11082-024-06882-x
12. A. S. Khalifa, N. M. Badra, H. M. Ahmed, W. B. Rabie, Retrieval of optical solitons in fiber Bragg gratings for high-order coupled system with arbitrary refractive index, *Optik*, **287** (2023), 171116. https://doi.org/10.1016/j.ijleo.2023.171116
13. Q. Zhou, Q. Zhu, A. Biswas, Optical solitons in birefringent fibers with parabolic law nonlinearity, *Opt. Appl.*, **44** (2014), 399–409. https://doi.org/10.5277/oa140305
14. L. Cheng, Y. Zhang, W. X. Ma, An extended (2+1)-dimensional modified Korteweg-de Vries–Calogero–Bogoyavlenskii–Schiff equation: Lax pair and Darboux transformation, *Commun. Theor. Phys.*, **77** (2024), 035002. https://doi.org/10.1088/1572-9494/ad84d3
15. J. Ahmad, S. Akram, S. U. Rehman, N. B. Turki, N. A. Shah, Description of soliton and lump solutions to M-truncated stochastic Biswas–Arshed model in optical communication, *Results Phys.*, **51** (2023), 106719. https://doi.org/10.1016/j.rinp.2023.106719
16. M. Shakeel, N. A. Shah, J. D. Chung, Application of modified exp-function method for strain wave equation for finding analytical solutions, *Ain Shams Eng. J.*, **14** (2023), 101883. https://doi.org/10.1016/j.asej.2022.101883
17. W. X. Ma, M. Chen, Direct search for exact solutions to the nonlinear Schrödinger equation, *Appl. Math. Comput.*, **215** (2009), 2835–2842. https://doi.org/10.1016/j.amc.2009.09.024
18. W. X. Ma, J. H. Lee, A transformed rational function method and exact solutions to the (3+1)-dimensional Jimbo–Miwa equation, *Chaos Soliton. Fract.*, **42** (2009), 1356–1363. https://doi.org/10.1016/j.chaos.2009.03.043

19. A. Ankiewicz, N. Akhmediev, Higher-order integrable evolution equation and its soliton solutions, *Phys. Lett. A*, **378** (2014), 358–361. https://doi.org/10.1016/j.physleta.2013.11.031

20. A. Ankiewicz, Y. Wang, S. Wabnitz, N. Akhmediev, Extended nonlinear Schrödinger equation with higher-order odd and even terms and its rogue wave solutions, *Phys. Rev. E*, **89** (2014), 012907. https://doi.org/10.1103/PhysRevE.89.012907

21. O. G. Gaxiola, A. Biswas, Y. Yildirim, A. S. Alshomrani, Bright optical solitons for the concatenation model with power-law nonlinearity: Laplace-Adomian decomposition, *Contemp. Math.*, 2023, 1234–1248. https://doi.org/10.37256/cm.4420233705

22. A. Biswas, J. V. Guzman, A. H. Kara, S. Khan, H. Triki, O. G. Gaxiola, et al., Optical solitons and conservation laws for the concatenation model: Undetermined coefficients and multipliers approach, *Universe*, **9** (2023), 15. https://doi.org/10.3390/universe9010015

23. H. Triki, Y. Sun, Q. Zhou, A. Biswas, Y. Yıldırım, H. M. Alshehri, Dark solitary pulses and moving fronts in an optical medium with the higher-order dispersive and nonlinear effects, *Chaos Soliton. Fract.*, **164** (2022), 112622. https://doi.org/10.1016/j.chaos.2022.112622

24. M. Y. Wang, A. Biswas, Y. Yıldırım, L. Moraru, S. Moldovanu, H. M. Alshehri, Optical solitons for a concatenation model by trial equation approach, *Electronics*, **12** (2023), 19. https://doi.org/10.3390/electronics12010019

25. S. Kumar, S. K. Dhiman, Lie symmetry analysis, optimal system, exact solutions and dynamics of solitons of a (3+1)-dimensional generalised BKP-Boussinesq equation, *Pramana-J. Phys.*, **96** (2022), 31. https://doi.org/10.1007/s12043-021-02269-9

26. H. Kumar, A. Malik, F. Chand, Analytical spatiotemporal soliton solutions to (3+1)-dimensional cubic-quintic nonlinear Schrödinger equation with distributed coefficients, *J. Math. Phys.*, **53** (2012), 103704. https://doi.org/10.1063/1.4754433

27. H. Bulut, T. A. Sulaiman, H. M. Baskonus, On the new soliton and optical wave structures to some nonlinear evolution equations, *Eur. Phys. J. Plus*, **132** (2017), 459. https://doi.org/10.1140/epjp/i2017-11738-7

28. E. M. Zayed, A. G. A. Nowehy, M. E. Elshater, Solitons and other solutions to nonlinear Schrödinger equation with fourth-order dispersion and dual power law nonlinearity using several different techniques, *Eur. Phys. J. Plus*, **132** (2017), 1–4. https://doi.org/10.1140/epjp/i2017-11527-4

29. K. K. Ahmed, H. M. Ahmed, N. M. Badra, M. Mirzazadeh, W. B. Rabie, M. Eslami, Diverse exact solutions to Davey–Stewartson model using modified extended mapping method, *Nonlinear Anal.-Model.*, **29** (2024), 983–1002. https://doi.org/10.15388/namc.2024.29.36103

30. M. A. S. Murad, Formation of optical soliton wave profiles of nonlinear conformable Schrödinger equation in weakly non-local media: Kudryashov auxiliary equation method, *J. Opt.*, 2024. https://doi.org/10.1007/s12596-024-02110-7

31. A. S. Khalifa, H. M. Ahmed, N. M. Badra, W. B. Rabie, F. M. A. Askar, W. W. Mohammed, New soliton wave structure and modulation instability analysis for nonlinear Schrödinger equation with cubic, quintic, septic, and nonic nonlinearities, *AIMS Math.*, **9** (2024), 26166–26181. https://doi.org/10.3934/math.20241278

32. A. Biswas, J. V. Guzman, Y. Yıldırım, L. Moraru, C. Iticescu, A. A. Alghamdi, Optical solitons for the concatenation model with differential group delay: Undetermined coefficients, *Mathematics*, **11** (2023), 2012. https://doi.org/10.3390/math11092012
33. M. S. Ullah, M. Z. Ali, H. O. Roshid, Bifurcation, chaos, and stability analysis to the second fractional WBBM model, *PLoS One*, **19** (2024), e0307565. https://doi.org/10.1371/journal.pone.0307565
34. M. Eslami, Exact traveling wave solutions to the fractional coupled nonlinear Schrödinger equations, *Appl. Math. Comput.*, **285** (2016), 141–148. https://doi.org/10.1016/j.amc.2016.03.032
35. R. Khalil, M. Al Horani, A. Yousef, M. Sababheh, A new definition of fractional derivative, *J. Comput. Appl. Math.*, **264** (2014), 65–70. https://doi.org/10.1016/j.cam.2014.01.002
36. Z. Yang, B. Y. Hon, An improved modified extended tanh-function method, *Z. Naturforsch. A*, **61** (2006), 103–115. https://doi.org/10.1515/zna-2006-3-401
37. M. Ekici, C. A. Sarmaşık, Various dynamic behaviors for the concatenation model in birefringent fibers, *Opt. Quant. Electron.*, **56** (2024), 1342. https://doi.org/10.1007/s11082-024-07252-3
38. E. U. Ekici, H. Triki, Stochastic perturbation of analytical solutions for the dispersive concatenation model with spatio-temporal dispersion having multiplicative white noise, *Nonlinear Dynam.*, **113** (2025), 4325–4353. https://doi.org/10.1007/s11071-024-10560-8